Transcriptome-wide analysis of the response of the thecosome pteropod Clio pyramidata to short-term CO2 exposure

Article *in* Comparative Biochemistry and Physiology Part D Genomics and Proteomics · June 2015

DOI: 10.1016/j.cbd.2015.06.002 · Source: PubMed

3 authors, including:

AE Maas
Bermuda Institute of Ocean Sciences
16 PUBLICATIONS **133** CITATIONS
SEE PROFILE

Ann M Tarrant
Woods Hole Oceanographic Institution
65 PUBLICATIONS **888** CITATIONS
SEE PROFILE

Transcriptome-wide analysis of the response of the thecosome pteropod *Clio pyramidata* to short-term CO_2 exposure

Amy E. Maas[1,2*], Gareth L. Lawson[1], and Ann M. Tarrant[1]

1. Biology Department, Woods Hole Oceanographic Institution, Woods Hole, MA 02543, USA
2. Current address: Bermuda Institute of Ocean Sciences, St. George's GE01, Bermuda

*Corresponding author e-mail: amy.maas@bios.edu.

Abstract

Thecosome pteropods, a group of calcifying holoplanktonic molluscs, have recently become a research focus due to their potential sensitivity to increased levels of anthropogenic dissolved CO_2 in seawater and the accompanying ocean acidification. Some populations, however, already experience high CO_2 in their natural distribution during diel vertical migrations. To achieve a better understanding of the mechanisms of pteropod calcification and physiological response to this sort of short duration CO_2 exposure, we characterized the gene complement of *Clio pyramidata*, a cosmopolitan diel migratory thecosome, and investigated its transcriptomic response to experimentally manipulated CO_2 conditions. Individuals were sampled from the Northwest Atlantic in the fall of 2011 and exposed to ambient conditions (~380 ppm) and elevated CO_2 (~800 ppm, similar to levels experienced during a diel vertical migration) for ~10 hrs. Following this exposure the respiration rate of the individuals was measured. We then performed RNA-seq analysis, assembled the *C. pyramidata* transcriptome *de novo*, annotated the genes, and assessed the differential gene expression patterns in response to exposure to elevated CO_2. Within the transcriptome, we identified homologs of genes with known roles in biomineralization in other molluscs, including perlucin, calmodulin, dermatopontin, calponin, and chitin synthases. Respiration rate was not affected by short-term exposure to CO_2. Gene expression varied greatly among individuals, and comparison between treatments indicated that *C. pyramidata* down-regulated a small number of genes associated with aerobic metabolism and up-regulated genes that may be associated with biomineralization, particularly collagens and C-type lectins. These results provide initial insight into the effects of short term CO_2 exposure on these important planktonic open-ocean calcifiers, pairing respiration rate and the gene expression level of response, and reveal candidate genes for future ecophysiological, biomaterial and phylogenetic studies.

Keywords: acidification, climate change, gastropod, lectin, mollusc, RNA-seq, transcriptomics

Introduction

The dissolution of anthropogenic carbon dioxide (CO_2) into seawater, or ocean acidification (OA), stands to impact a broad variety of marine organisms, especially those that secrete calcium carbonate ($CaCO_3$) shells or skeletons (Fabry et al., 2008). As CO_2 equilibrates into seawater, pH and the concentration of carbonate ions decrease, causing $CaCO_3$ to dissociate and affecting the ability of calcifying animals to create and maintain calcareous structures (Gattuso et al., 1999; Riebesell et al., 2000). Furthermore, decreasing pH in the water alters the acid-base balance of the intra- and extracellular fluids of marine organisms (Miles et al., 2007; Seibel and Fabry, 2003; Seibel and Walsh, 2001). Since CO_2 is produced naturally as a byproduct of respiration, all organisms have physiological mechanisms for maintaining internal cellular pH. These compensatory mechanisms may, however, cease to function if internal acidosis becomes too severe over short time scales and generally fail over extended periods of internal pH imbalance. Classical organismal-level metrics (e.g., metabolic rate, calcification, mortality) have revealed a complex pattern of intra- and inter-specific variation in responses to CO_2 exposure (reviewed in Hendriks et al., 2010; Kroeker et al., 2013; Kroeker et al., 2010). The variability in these responses, and their dependence on duration of exposure or co-varying stressors, suggest that there is an energetic cost associated with compensating for high CO_2 (e.g., Cummings et al., 2011; Langenbuch and Pörtner, 2004; Stumpp et al., 2011b).

One group thought to be particularly sensitive to OA is the thecosomatous (i.e., shelled) pteropods. These holoplanktonic gastropods, related to terrestrial snails and also known as sea butterflies, produce thin shells made of aragonite, a highly soluble form of $CaCO_3$. In temperate and polar seas, thecosomes can become a numerically dominant member of the zooplankton community (Hunt et al., 2008). This causes them to be significant consumers of primary production, serve as a key food item for commercially important fish, seabirds and whales, and substantially contribute to carbon flux to the deep ocean (reviewed in: Bednaršek et al., 2012a; Lalli and Gilmer, 1989; Manno et al., 2010). Studies of thecosome biomineralization have revealed that increasing CO_2 levels result in decreased calcification and shell degradation (Bednaršek et al., 2014; Bednaršek et al., 2012b; Comeau et al., 2009; Lischka and Riebesell, 2012; Manno et al., 2012). It remains unclear whether the decreases in calcification documented in thecosomes at high CO_2 concentrations are a result of their inability to form carbonates, or rather are a result of a re-allocation of energy, as has been described in other species (e.g., Melzner et al., 2013; Stumpp et al., 2012).

The impact of CO_2 on the metabolic rate and mortality of thecosome pteropods has been shown to be variable, and highly dependent upon the presence of co-varying stressors such as salinity, temperature and feeding history (Comeau et al., 2010a; Lischka and Riebesell, 2012; Maas et al., in review; Manno et al., 2012; Seibel et al., 2012). In contrast to laboratory findings concerning the effects of under-saturation on pteropods, Maas et al. (2012) found that some species of thecosomes regularly experience conditions of high CO_2 and aragonite saturation states <1 during diel vertical migrations into an oxygen minimum zone in the eastern tropical North

Pacific, and do not respond to short-term laboratory CO_2 exposure with a change in metabolic rate. This suggests that in some thecosome species there is a potential adaptation or acclimation to high CO_2, at least over short periods. Supporting this idea, more recent work comparing thecosomes from the Northeast Pacific and Northwest Atlantic revealed that the metabolic rates of multiple thecosome pteropod species are not affected by short-term exposure to CO_2 at the levels predicted for the coming century (800 ppm; Maas et al., in review). Exploring the physiological mechanisms these species use to cope with short-term CO_2 exposure may provide insight into what duration and level of exposure to anthropogenic CO_2 thecosomes can tolerate. Elucidating these mechanisms will also provide a means to characterize the physiological condition of pteropods within natural populations and enable development of molecular biomarkers indicating responses to elevated CO_2 exposure.

An increasing number of studies have employed molecular methods to disentangle the complex picture associated with CO_2 response, revealing changes in expression of genes with a known or predicted role in acid-base balance, apoptosis, biomineralization, development, protein synthesis, energetic metabolism, and stress responses (Hüning et al., 2013; Kaniewska et al., 2012; Kurihara et al., 2012; Moya et al., 2012). For example, Moya et al. (2012) showed that coral larvae respond to CO_2 through changes in gene expression that were consistent with suppressed metabolism and changes in calcification. They also discovered an unexpected lack of response in ion transport proteins and a down-regulation of carbonic anhydrase genes. Relatively few studies have matched observations of altered gene expression with organismal-level observations such as developmental delays or changes in metabolic rate (e.g., Stumpp et al., 2011b). Many of the previous studies have used quantitative PCR (qPCR), a targeted approach which involves picking a small number of genes *a priori* such as studies with mussel (Hüning et al., 2013), abalone (Zippay and Hofmann, 2010), urchin (Stumpp et al., 2011a), and oyster (Liu et al., 2012), or using microarrays, which have historically only been done with well-studied organisms such as urchins (Evans et al., 2013; O'Donnell et al., 2010; Todgham and Hofmann, 2009) and corals (Kaniewska et al., 2012).

Despite the benefits of using gene expression studies for understanding the response to CO_2 at a mechanistic level, there have been no published studies of pteropod gene expression to date. High throughput RNA sequencing (RNA-seq) methods enable quantitative characterization of gene expression patterns across the transcriptome (Ekblom and Galindo, 2011; Vijay et al., 2012). When a reference genome is not available, a transcriptome can be assembled *de novo* from millions of short reads. The reads from individual samples can then be mapped onto this reference transcriptome for a comprehensive assessment of differential gene expression. Furthermore, once a transcriptome has been assembled, it can serve as a resource for targeted analyses of individual genes. In the context of ocean acidification, these targeted analyses may include the identification of pteropod homologs of genes associated with calcification in other mollusc species.

A number of recent papers have focused on the characterization of biomineralization proteins and genes in molluscs (Gardner et al., 2011; Jackson et al., 2010; Joubert et al., 2010; Shi et al., 2012; Zhang and Zhang, 2006; Zhao et al., 2012a), while other studies have increased the number of available molluscan transcriptomes to include pearl oysters (Huang et al., 2012; Zhao et al., 2012a; Zhao et al., 2012b), sea hares (Fiedler et al., 2010; Heyland et al., 2011), freshwater snails (Sadamoto et al., 2012), abalone (Franchini et al., 2011; Picone et al., 2015), scallops (Artigaud et al., 2014), mussels (Freer et al., 2014), and clams (Clark et al., 2010; Sleight et al., 2015). These studies confirm that molluscan biomineralization is a complex process with some conserved pathways shared between distantly related animal groups, and other proteins and compounds that are taxonomically restricted (Jackson et al., 2010), as has been shown in more distantly related animal groups (Jackson et al., 2007; Moya et al., 2012; Moya et al., 2008). Comparing the transcriptomic underpinnings of shell accretion in thecosomes with those in other molluscs may thus provide a useful contrast because of the different ecological pressures of a holoplanktonic lifestyle and the structures and processes associated with building a calcium carbonate shell principally (> 50%) comprised of aragonite (Bé and Gilmer, 1977). Beyond understanding the mechanism of calcification to explore the specific effects of climate change on shell formation, biomineralization in the molluscan lineage may thus also be interesting from a material properties and evolutionary standpoint (Jackson et al., 2010; Xie et al., 2011).

In this study, we focus on *Clio pyramidata* (Linnaeus, 1767), a common circumglobal species that has a multilayered aragonite shell, and is known to migrate vertically on a diel basis into regions of high CO_2 in some ocean basins (Maas et al., 2012). As in most thecosomes, the growth sequence and processes of biomineralization for this species are poorly-characterized and no gene sequences beyond the barcoding regions were known. In this study, we have assembled and annotated a *de novo* transcriptome for *C. pyramidata*. To characterize the transcriptome, and to gain insight into the effects of short-term CO_2 exposure (similar to what would be experienced during a diel migration), we then exposed *C. pyramidata* to ambient or elevated CO_2 concentrations, measured respiration rate, and used RNA-seq to test for changes in gene expression. By pairing these two metrics we hoped to shed light on the lack of a significant effect of CO_2 exposure on *C. pyramidata* oxygen consumption rates that has been observed previously in similar metabolic experiments in the Pacific (Maas et al., 2012). Specifically, transcriptional profiling was used to investigate whether this lack of response to short term CO_2 exposure is due to an absence of physiological stress, or is rather a product of the redistribution of energetic resources.

Materials and Methods:

Animal Collection and Experimental Setup:

C. pyramidata were collected from the R/V *Oceanus* in August 2011 at an off-shelf station east of the Grand Banks in the Northwest Atlantic (44.94°N, 42.00°W). Animals were captured using

a 1 m diameter, 150 µm mesh, Reeve net. *Clio pyramidata* are small, relatively rare, difficult to capture without damaging, and hard to maintain in shipboard conditions, limiting the numbers available for experimentation. Individuals for this experiment were collected from the same net tow to minimize pre-existing environmental variability and handling differences between tows (hydrographic data and tow details in Supplementary File 1). *Clio pyramidata* from this tow were placed in open jars of locally collected filtered seawater (33 psu) at 15°C in temperature-controlled waterbaths at densities < 15 individuals L^{-1} for 12 h (± 30 min) to allow for gut clearance. This temperature and salinity were chosen as individuals of this species had recently been sampled under these conditions.

CO_2 Exposures and Respiration Experiments

After the gut clearance period, healthy individuals (swimming and with intact shells) were selected for closed chambered respiration experiments using a Clarke-type oxygen electrode method (Maas et al., 2012; Marsh and Manahan, 1999). Individuals were placed in separate 20 mL air-tight glass chambers with 0.2 micron filtered seawater. The experimental water (33 psu) had previously been bubbled in 1 L batches for 45-60 minutes with ambient air (~380 ppm CO_2) or a certified gas mixture containing 800 ppm CO_2 (± 2 %, Corp Brothers; 21% oxygen, balanced with nitrogen). This treatment was applied to simulate projected levels for the open ocean in the year 2100 (A2 emissions scenario, I.P.C.C., 2007) and is a level that *C. pyramidata* is known to currently experience in other portions of its distribution (i.e., the North Pacific). The water contained 25 mg L^{-1} each of streptomycin and ampicillin to prevent bacterial growth, a procedure that has been shown to have no effect on the respiration rate of thecosome pteropods (Howes et al., 2014).

For every 3 experimental glass chambers, another control glass chamber was set up with the same water but without an animal to enable monitoring of background bacterial respiration. Respiration chambers were maintained at temperature in a waterbath during experimental incubations, after which the oxygen saturation in the chamber was measured. Duration of exposure varied slightly due to the sequential measurement of O_2 concentration in successive chambers at the beginning and end of the experiments, but CO_2 exposures were between 9.5-10 hours for the high treatment and 10.25-10.75 h for the ambient treatment (to replicate diel vertical migratory periods). For each measurement, an aliquot of water was withdrawn using an airtight 500 µL Hamilton syringe and injected past a Clarke-type microcathode (part #1302, Strathkelvin Instruments, North Lanarkshire, United Kingdom), which was attached to an O_2 meter (part #782) in a water-jacketed injection port (part #MC100), and the reading was allowed to stabilize for at least 30 seconds prior to being recorded. At the conclusion of the experiments, oxygen in the chambers remained between 73-96% of saturation, above the critical oxygen partial pressure typical of marine animals (Childress and Seibel 1998). The animals were then removed from the chamber, blotted dry, and frozen in liquid nitrogen. Total handling time of

organisms during the final O_2 measurements was ~10 min per respiration experiment, with less than a minute between removal from the chamber and preservation to minimize handling stress.

The same individuals used in the study of oxygen consumption were stored at -80°C for transcriptomic analysis. Prior to RNA extraction, individuals were quickly weighed on a microbalance (+/- 0.0001 g) to allow for the calculation of their mass specific O_2 consumption rate (µmoles g^{-1} h^{-1} wet weight). Tissue was then dissected from the shell to avoid both the possible pH interference due to the calcium carbonate of the structure and contamination by other taxa trapped in the shell. Statistical analysis of respiration rate was conducted using a general linear model in SPSS on log-transformed oxygen consumption, with treatment as the random factor and log-transformed wet mass as a covariate.

Carbonate Chemistry

DIC measurements were taken after each experiment from control syringes that had been allowed to come to room temperature (>6 h) before analysis. DIC samples were analyzed on a DIC auto-analyzer (AS-C3, Apollo SciTech, Bogart, USA) via acidification, followed by non- dispersive infrared CO_2 detection (LiCOR 7000: Wang et al., 2013a; Wang and Cai, 2004). Samples were measured a minimum of three times to obtain replicate measurements. The instrument was calibrated with certified reference material (CRM) from Dr. A.G. Dickson at the Scripps Institution of Oceanography and has a precision and accuracy of ± 2.0 µmol kg^{-1}. Best practices for calculating carbonate chemistry (Riebesell et al., 2010) include measurement of two of the CO_2 system parameters. Due to the small volumes of water in the experimental chambers it was not possible to measure both DIC and total alkalinity simultaneously from the control syringes, and instead total alkalinity of batches of water (collected weekly) was measured using an Apollo SciTech alkalinity auto-titrator, a Ross combination pH electrode, and a pH meter (ORION 3 Star) based on a modified Gran titration method (Wang et al., 2013b). These batches of water were then used for multiple experiments over the course of several days. Unfortunately, the alkalinity changed over time, likely due to microbial activity, and measurements proved not to have been taken at sufficient temporal resolution to constrain the carbonate chemistry within this experiment using total alkalinity. Subsequent diffusion calculations, however, indicated that the 45 - 60 min bubbling was sufficient to fully achieve the targeted pCO_2 levels. As such we used the manufacturer's certification of pCO_2 within the gas mixture as our second parameter to characterize the carbonate system. Other carbonate system parameters, including aragonite saturation state, were calculated using the CO2SYS software (Pierrot et al., 2006), the carbonic acid dissociation constants by Mehrbach et al. (1973), refitted by Dickson and Millero (1987), and the $KHSO_4$ dissociation constant from Dickson (1990). The ± 2% error in CO_2 concentration reported by the gas supplier was incorporated into the calculations of the carbonate chemistry to characterize uncertainty.

RNA Extraction and Illumina Sequencing

RNA was extracted from individuals with either the Aurum Total RNA Fatty and Fibrous Tissue Kit (BioRad) or the E.Z.N.A. Mollusc RNA Kit (Omega Biotek) and eluted in 25-40 µL molecular biology grade water. Both methods yielded one sharp band of RNA with no signs of degradation on a denaturing agarose gel and on a Bioanalyzer profile. This indicates that pteropods, like some other protostomes, likely have a delicate 28S ribosomal RNA strand that breaks during extraction, making a traditional quality score relatively uninformative (Gayral et al., 2011; Winnebeck et al., 2010).

RNA extracts from four individuals per treatment (8 individuals in total, A-D exposed to elevated CO_2, E-H exposed to ambient) were chosen based on RNA quality and yield. RNA was submitted to the Genomic Sequences Laboratory of Hudson Alpha for library construction and sequencing. Libraries were constructed using Tru-Seq RNA Sample Prep Kits, multiplexed, and sequenced in duplicate on two lanes of the Illumina HiSeq platform (v. 1.9) as 50 base pair (bp) paired-end reads.

Assembly and Annotation

Raw sequences were quality filtered and assembled into transcripts *in silico*. The resulting transcripts were annotated to indicate their similarity to genes with known function. To accomplish this, adapter sequences and bases with a phred quality score below 30 were first removed using Trimmomatic (Lohse et al., 2012). *De novo* transcriptome assembly was performed with Trinity (version r2013-02-25: Grabherr et al., 2011) using a pooled file of all reads from both treatments and the default parameters (minimum contig length: 200, k-mer length 25). The assembled transcripts were imported into Blast2GO (Conesa et al., 2005), where those > 200 bp were compared to the SWISS-PROT database using BLASTX with an e-value $<1.0\ e^{-6}$ to remain relatively consistent with other recent non-model marine transcriptomes (i.e., Burns et al., 2013; Craft et al., 2010; de Wit and Palumbi, 2013; Harms et al., 2013). These transcripts were further annotated using the Blast2GO program that assigned Gene Ontology (GO) terms for those with an e-value $<1.0\ e^{-10}$ to reduce the probability of mis-annotation (du Plessis et al., 2011).

Analysis of Biomineralization Genes

To specifically search for transcripts associated with biomineralization, we utilized the recent annotation of the oyster genome, which includes both a set of genes that were either highly or differentially expressed in shell mantle tissue and a comparison of oyster genes with sequences known to be associated with shells in other molluscs (Zhang et al., 2012). We assembled a BLAST database using the Genbank accession numbers for these mantle and biomineralization proteins. We then conducted a TBLASTN search to find putative homologs of these genes within the *C. pyramidata* transcriptome (e-value $<1.0\ e^{-6}$). Transcripts of interest, such as those that showed homology to perlucin sequences in the molluscan biomineralization database were again used to query the NCBI non-redundant database (nr) using BLASTX as implemented in

Blast2GO. The sequences exhibiting greatest similarity to annotated perlucin sequences (five sequences with lowest e-values) were translated *in silico* using the ExPASy translate tool (Artimo et al., 2012). Stop codons were trimmed, and then these sequences were aligned with annotated perlucin protein sequences from other molluscs using MUSCLE (Edgar, 2004). These included the perlucin sequences that have been shown to be associated with biomineralization in the triangle sail mussel (*Hyriopsis cumingii*, GenBank KC436008: Lin et al., 2013), the abalone (*Haliotis laevigata,* P82596.3: Mann et al., 2000), and from the disk abalone (*Haliotis discus discus*, ABO26590.01: Wang et al., 2008). Also included in the alignment was the C-type lectin from the bay scallop that appears to be associated with immune response (*Argopecten irradians*, ADL27440.1 Mu et al., 2012), as well as sequences inferred *in silico* such as the perlucin sequences associated with the Pacific oyster (*Crassostrea gigas*, EKC39512.1: Zhang et al., 2012) and the abalone (*Haliotis diversicolor*, AEQ16377.1) and the C-type lectins from the pearl oyster (*Pinctada fucata*, ACO36046.1) and the clam (*Ruditapes philippinarum*, ACU83213).

Differential Expression

The reads from each library were pooled and separately mapped to our reference transcriptome using Bowtie (Langmead et al., 2009) via the RSEM script that is associated with the Trinity package set with default parameters (Haas et al., 2013). To compare overall gene expression patterns among individuals prior to identifying differentially expressed genes, we used the statistical package Primer (Clarke and Gorley, 2006) to construct a Bray-Curtis similarity matrix of the standardized edgeR normalized (TMM, trimmed mean of M-values; Robinson and Oshlack, 2010) fragments per kilobase per million reads mapped (FPKM) transcript counts of all genes (Trinity components) expressed in at least two individuals (to reduce variability caused by rare transcripts). The edgeR package was then used to identify genes (Trinity components) that exhibited significant differences in expression between the two CO_2 treatments (Robinson et al., 2010). Results were reported as significant when the change in $\log_2$-transformed gene expression was greater than two (corresponding to a four-fold change in expression) and the p-value and false discovery rate were < 0.05. These differentially expressed genes were re-annotated using a BLASTX against the NCBI non-redundant (e-value $<1.0\ e^{-3}$) and Interpro (Hunter et al., 2011) databases.

Results

Consistent with experiments conducted in other ocean basins (Maas et al., in review; Maas et al., 2012), wild caught *C. pyramidata* from the Northwest Atlantic that were exposed to either ambient (~380 ppm) or elevated (~800 ppm) CO_2 for ~10 h, simulating the timing of exposure associated with diel vertical migration, showed no significant difference in respiration rate. Using these same experimental individuals, libraries were sequenced from eight pteropods (4 per treatment) using Illumina HiSeq technology. These libraries were used to build a reference transcriptome for *C. pyramidata* that revealed a number of biomineralization-associated genes similar to those found in other molluscan lineages. Only a small number of genes exhibited

significant changes in expression in association with short-term exposure to moderately elevated CO_2.

Respiration Experiments and Carbonate Chemistry

The experimental CO_2 exposure achieved an aragonite saturation state (ΩAr) of 2.44 and pH of 8.06 in the ambient treatment (380 ppm CO_2) and an ΩAr of 1.41 and pH of 7.78 (800 ppm CO_2) in the elevated treatment (Table 1). Incorporating the uncertainty in pCO_2 based on the manufacturer's certification of the gas mixture, we calculated a potential error of ± 0.03 in ΩAr and ± 0.01 in pH for the 800 ppm treatment; thus our treatments were near the targeted values and achieved the desired result of acutely different exposure conditions. There were no significant differences in the respiration rate of individuals from the two treatments; this also remained true when considering a larger sample size of individuals from more sample locations in the Atlantic as well as from the Pacific Ocean (Fig. 1). There were no significant differences between the treatments within the Atlantic ($F_{1,14} = 0.037$, $p = 0.850$), nor when individuals from the Pacific were included in the analysis ($F_{1,42} = 0.540$, $p = 0.466$).

Assembly and Annotation

Sequencing resulted in ~50 million reads per individual after quality trimming. The assembled transcriptome contained 30,800 components ("genes") and 45,739 transcripts ("isoforms") greater than 200 bp, an average transcript length of 618 bp, and an N50 of 852 bp. We were able to annotate 9,280 of the transcripts (20%) based on similarity to genes within the SWISS-PROT database using an e-value cut-off of $1.0\ e^{-6}$. The percent of annotated sequences was positively correlated with transcript length; however, we were still unable to identify 70% of the longest sequences (>2,000 bp). Gene ontology (GO) terms were assigned to 7,989 of the transcripts with significant BLAST hits (86%).

Candidate biomineralization-associated transcripts

A number of genes that have previously been shown to be involved with biomineralization have potential homologs within the pteropod transcriptome. Queries of the pteropod transcriptome with 45 biomineralization-associated genes from other molluscs resulted in identification of 831 *C. pyramidata* transcripts. These included 13 transcripts that were annotated as carbonic anhydrase precursors, 59 as calmodulin or calmodulin-like proteins, 10 chitin synthases, and surprisingly 282 transcripts annotated as perlucin (Supplementary File 2). In addition, we identified 56 transcripts through queries with 23 sequences that were up-regulated in oyster mantle (Zhang et al., 2012). Transcripts that showed homology to perlucin sequences in the molluscan biomineralization database were BLASTed against the nr database to help provide a list of the most likely perlucin candidates. When translated, the top five matches (based on e-value) aligned well with previously identified perlucin transcripts from various other molluscs (Fig. 3), revealing the six highly conserved cystine residues, the residues putatively involved in calcium-dependent carbohydrate binding (Mann et al., 2000) and the motifs proposed to

determine carbohydrate-binding specificity for galactose (QPD) binding (Iobst and Drickamer, 1994).

Differential expression

There was a high degree of variability in overall transcript expression patterns among individuals (20-80% similarity in pairwise comparisons, Fig. 2). Between treatments 29 genes were differentially expressed, four of which were down-regulated in high CO_2 and the rest of which were up-regulated (Table 2). Of the four genes that were down-regulated in individuals exposed to high CO_2, two were annotated: both were associated with the mitochondrial inner-membrane complex (cytochrome c oxidase subunit I and III), however there was high variability in their expression levels within treatments. Of the 29 genes that were up-regulated only six could be annotated through BLASTX searches of the NCBI non-redundant database and an InterPro Scan. Two of these were associated with carbohydrate binding of the C-type lectin family (conglutinin and a lactose-binding lectin that was also identified as being a perlucin homolog), one was associated with protein binding, another with the regulation of transcription via DNA binding, another with hydrolase activity in an extracellular region, and the final was a chymotrypsin-like elastase (Table 2).

Discussion

The sequences generated by this *de novo* transcriptome assembly provide a first glimpse into the gene complement of a thecosome pteropod, revealing a number of transcripts that are putative homologs of genes involved in biomineralization in other molluscs. The respiration rate experiments show no effect of short term CO_2 exposure, a finding that is also consistent with the very small number of candidate genes that were identified in the differential expression analysis. The candidate genes that may respond to pH conditions replicating exposures and durations comparable to a diel vertical migration include those associated with biomineralization and aerobic metabolism, although these results should be interpreted cautiously and require validation with a larger dataset.

Assembly and Annotation

Comparison of the *de novo* thecosome pteropod transcriptome with the SWISS-PROT database resulted in annotation of ~20% of the 45,739 transcripts. This relatively low percentage of identified transcripts is within the range of other recent assemblies of transcriptomes from non-model marine invertebrates, all of which were annotated using the NCBI non-redundant database (19-37%, spider crab (Harms et al., 2013), coral (Meyer et al., 2011), krill (Clark et al., 2011), amphipod (Zeng et al., 2011), abalone (de Wit and Palumbi, 2013), brittle star (Burns et al., 2013). Use of SWISS-PROT, a highly-curated and more restricted database, rather than the NCBI non-redundant database, which has greater species coverage, was selected to achieve more informative annotation. Thus, as in other studies, low identification is likely due to the relatively

small available database of annotated genes from closely-related species, typical in the study of non-model organisms.

Biomineralization

Queries of the pteropod transcriptome with bivalve biomineralization transcripts revealed a large number of potential homologs including dermatopontin, calmodulin, calponin, chitin synthases and carbonic anhydrase precursors, providing a useful resource for future exploration of these gene families. There were also a number of genes for which the annotation corresponded to as-yet undescribed transcripts associated with shell mantle expression in oyster. The highest number of transcripts found via our search, however, belonged to a group of C-type lectin domain proteins that are similar to perlucin. We identified five likely perlucin homologs, which would be the best first choices to further explore this gene family in pteropods. Perlucin, a water-soluble non-acidic protein with a calcium-dependent carbohydrate binding domain has been shown to be important for shell biomineralization in the nacreous (aragonitic) layer of the abalone *Haliotis laevigata* (Mann et al., 2000), and in the freshwater pearl mussel *Hyriopsis cumingii* (Lin et al., 2013). Perlucin-like genes have also been found to be strongly expressed in the outer mantle tissue of the mussel *Mytilus edulis* (Freer et al., 2014; Hüning et al., 2012). The abalone perlucin protein has been described through functional studies as a promoter of calcium carbonate precipitation, as the site of nucleation for calcium carbonate crystallization, and as a modifier of crystal morphology (Blank et al., 2003; Weiss et al., 2000). A recombinant perlucin gene from the abalone *Haliotis discus discus* has been shown to promote the growth of calcium carbonate crystals in *E. coli* (Wang et al., 2010). The C-type lectin domain proteins also can have an immune function in molluscs (Mu et al., 2012; Yang et al., 2011), and it has been hypothesized that some perlucin-like sequences may have an immune function (Venier et al., 2011; Wang et al., 2008). If the pteropod perlucin-like sequences are associated with shell healing or repair, their induction could be an important physiological pathway for pteropods in the response to high CO_2.

Interestingly, as was found during annotation of the oyster genome, a number of different transcripts were frequently identified as putative homologs of a single sequence. This was particularly evident for perlucin, where all 282 genes were identified as being homologs of only 4 abalone sequences, each which were described as either perlucin or perlucin-like genes. Since the perlucin-like C-type lectins appear to have diversified within the lineage leading to *C. pyramidata*, further investigation of the evolution of C-type lectins within pteropods should be a priority for further study. Similarly, the large number of paralogous biomineralization genes in the oyster genome was suggested by Zhang et al. (2012) to be a consequence of rapid diversification and strong selection pressure, which is thought to underlie the evolutionary history of shell related genes. It is interesting that rapid diversification may have occurred independently in the highly derived holoplanktonic pteropods, emphasizing the usefulness of this species for comparative studies of biomineralization.

Differential Expression

We found high variability in gene expression among individual pteropods, likely due to the fact that samples were generated from wild-caught individuals, which may have included differences in genetic background, physiological condition and size. It is also important to note that, because these are small animals, analysis was done with whole organisms, rather than specific tissues, which may dampen signals from specialized tissues such as the biomineralizing mantle. In the context of this high variability, the limitation of whole animal extractions, and the low number of biological replicates, the small subset of genes that were differentially expressed as a consequence of exposure to high CO_2 should be considered with caution and requires further confirmation, including further exploration of gene expression patterns with qPCR. Due to the rarity and small size of the organisms, we did not have enough remaining material from these experiments to validate our findings concerning differential expression reliably through qPCR measurements. In combination with a lack of effect on respiration rate (Maas et al., in review; Maas et al., 2012), however, the low number of differentially expressed genes suggests a lack of substantial physiological response to the experimental conditions.

Despite the limitations of the differential expression analyses, the present results nonetheless provide insight into transcripts that may be potentially influenced by short duration CO_2 exposure. The small number of annotated down-regulated genes in the high CO_2 treatment were highly variable in expression pattern and were associated with the mitochondrial inner membrane complex. Changes in mitochondrial inner membrane complex transcript abundance were also observed in urchins exposed to CO_2 in a longer duration developmental study (40 h) conducted by Todgham and Hofmann (2009) and in coral exposed to CO_2 for three days by Moya et al. (2012) and interpreted as being associated with a reduction in oxidative metabolism. Subunits of the downstream enzyme in the oxidative metabolism pathway, ATP synthase, have also been documented to be down-regulated in invertebrate models (mussels, Hüning et al., 2013; urchins, Todgham and Hofmann, 2009), emphasizing oxidative metabolism as an important molecular response to high CO_2. Those genes that were up-regulated had annotations that corresponded with the extracellular region and gene families known to be associated with biomineralization. These included putative homologs of perlucin, and conglutinin, which is a calcium-dependent collagen-containing lectin. Both conglutin and perlucin are C-type lectins. This diverse family is known to be associated both with innate immune response and with the biomineralization protein matrix (Mann et al., 2000; Mu et al., 2012; Wang et al., 2008). Moya et al. (2012) also found up-regulation of collagens and lectins in coral that had been exposed to elevated CO_2 conditions that were not corrosive to $CaCO_3$ structures (saturation state remained > 1). Other studies have seen patterns of down-regulation of transcript expression of collagens in urchins (Todgham and Hofmann, 2009) and both down- and up-regulation of transcript expression of C-type lectins, such as SM30 in urchins (Kurihara et al., 2012; Stumpp et al., 2011a). A qPCR-based study with species more closely related to pteropods (mussels) found no significant changes in a specific

perlucin-like C-type lectin (Hüning et al., 2013). Clearly, the complexity and diversity of the protein biomineralization matrix and its response to CO_2 exposure still bears further investigation across a diversity of taxa, including thecosome pteropods.

Conclusions

The species studied is a strong diel migrator that experiences conditions of high CO_2 in portions of its natural distribution, and was shown here to have no significant respiratory response to short-term, moderate CO_2 exposure. In conjunction with this lack of organismal-level response, the molecular response to this degree of exposure appeared to be limited to a small portion of the *C. pyramidata* transcriptome, with some of the identified transcripts being associated with the mitochondrial inner membrane complex, carbohydrate binding and the extracellular matrix/biomineralization. The analysis of biomineralization associated genes suggests a number of similarities with those of other molluscan calcifiers. The C-type lectin family, and the perlucin-like homologs in particular, merit further exploration both as a consequence of their abundance in the transcriptome and their likely role in calcification. The sequences and potential responses identified here thus pave the way for a detailed exploration of thecosome pteropod biomineralization. They also provide groundwork for further experimentation with larger scale experiments of individual- and population-level responses to longer term CO_2 stress at the molecular level, complementing the growing body of literature exploring metabolic, ecological, and calcification responses of these sentinel open-ocean calcifiers.

Data Accessibility

The NCBI Bioproject number for the data associated with this project is PRJNA231010. Raw sequence data was submitted to the NCBI Short Read Archive (SRA) under accession numbers GSM1283048–GSM1283055. This Transcriptome Shotgun Assembly project has been deposited at DDBJ/EMBL/GenBank under the accession GAWL00000000. The version described in this paper is the first version, GAWL01000000. Gene expression data was submitted to the NCBI Gene Expression Ombnibus (GEO) under the accession number GSE53151.

List of Abbreviations

base pair (bp), Basic Local Alignment Search Tool (BLAST), calcium carbonate ($CaCO_3$), carbon dioxide (CO_2), fragments per kilobase per million reads mapped (FPKM), Gene ontology (GO), General Linear Model (GLM), high throughput RNA sequencing (RNA-seq), National Center for Biotechnology Information (NCBI), ocean acidification (OA), quantitative polymerase chain reaction (qPCR), trimmed mean of M-values (TMM)

Acknowledgements

We would like to acknowledge the Captain and crew of the R/V *Oceanus*, and all the scientists, students and volunteers who participated in the OC473 expedition. We would also like to thank

Amalia Aruda Almada, Mike Brosnahan, Adam Reitzel, Leocadio Blanco Bercial and Santiago Herrera for their support, insight and input into methodologies, analysis and interpretation. The Extreme Science and Engineering Discovery Environment (XSEDE), which is supported by National Science Foundation grant number OCI-1053575, provided computing resources for the differential expression analysis. This material is based upon work supported by the National Science Foundation's Ocean Acidification Program under grant number OCE-1041068 (to Lawson, Wang, Lavery, and Wiebe), the Woods Hole Oceanographic Institution's Access to the Sea program (to Tarrant, Maas and Lawson) and the WHOI postdoctoral scholarship program (to Maas).

Author Contributions

Study design was initiated by all three authors. The animal collection and experimental manipulations were conducted by AEM and GLL. RNA processing and bioinformatics analysis were done by AEM and AMT. The initial draft was prepared by AEM, and all co-authors collaborated on data interpretation and manuscript revision.

References:

Artigaud, S., Thorne, M.A., Richard, J., Lavaud, R., Jean, F., Flye-Sainte-Marie, J., Peck, L.S., Pichereau, V., Clark, M.S., 2014. Deep sequencing of the mantle transcriptome of the great scallop *Pecten maximus*. Marine genomics 15, 3-4.

Artimo, P., Jonnalagedda, M., Arnold, K., Baratin, D., Csardi, G., De Castro, E., Duvaud, S., Flegel, V., Fortier, A., Gasteiger, E., 2012. ExPASy: SIB bioinformatics resource portal. Nucleic Acids Research 40, W597-W603.

Bé, A.W.H., Gilmer, R.W., 1977. A zoogeographic and taxonomic review of Euthecosomatous Pteropoda, in: A. Ramsay (Ed.), Oceanic Micropalaeontology. Academic Press, London, 733-808.

Bednaršek, N., Feely, R., Reum, J., Peterson, B., Menkel, J., Alin, S., Hales, B., 2014. *Limacina helicina* shell dissolution as an indicator of declining habitat suitability owing to ocean acidification in the California Current Ecosystem. Proceedings of the Royal Society B: Biological Sciences 281, 20140123.

Bednaršek, N., Možina, J., Vogt, M., O'Brien, C., Tarling, G., 2012a. The global distribution of pteropods and their contribution to carbonate and carbon biomass in the modern ocean. Earth System Science Data 4, 167-186.

Bednaršek, N., Tarling, G.A., Bakker, D.C.E., Fielding, S., Cohen, A., Kuzirian, A., McCorkle, D., Lézé, B., Montagna, R., 2012b. Description and quantification of pteropod shell dissolution: a sensitive bioindicator of ocean acidification. Global Change Biology.

Blank, S., Arnoldi, M., Khoshnavaz, S., Treccani, L., Kuntz, M., Mann, K., Grathwohl, G., Fritz M., 2003. The nacre protein perlucin nucleates growth of calcium carbonate crystals. Journa of microscopy 212, 280-291.

Burns, G., Thorndyke, M.C., Peck, L.S., Clark, M.S., 2013. Transcriptome pyrosequencing of the Antarctic brittle star *Ophionotus victoriae*. Marine Genomics 9, 9-15.

Clark, M., Thorne, M., Vieira, F., Cardoso, J., Power, D., Peck, L., 2010. Insights into shell deposition in the Antarctic bivalve *Laternula elliptica*: gene discovery in the mantle transcriptome using 454 pyrosequencing. BMC genomics 11, 362.

Clark, M.S., Thorne, M.A.S., Toullec, J.Y., Meng, Y., Peck, L.S., Moore, S., 2011. Antarctic krill 454 pyrosequencing reveals chaperone and stress transcriptome. PLoS ONE 6, e15919.

Clarke, K.R., Gorley, R.N., 2006. PRIMER v6: User Manual/Tutorial. PRIMER-E, Plymouth.

Comeau, S., Gorsky, G., Jeffree, R., Teyssie, J., Gattuso, J.P., 2009. Impact of ocean acidification on a key Arctic pelagic mollusc (*Limacina helicina*). Biogeosciences 6, 1877-1882.

Comeau, S., Jeffree, R., Teyssié, J.L., Gattuso, J.P., 2010a. Response of the Arctic pteropod *Limacina helicina* to projected future environmental conditions. PLoS One 5, e11362.

Conesa, A., Götz, S., García-Gómez, J.M., Terol, J., Talón, M., Robles, M., 2005. Blast2GO: a universal tool for annotation, visualization and analysis in functional genomics research. Bioinformatics 21, 3674-3676.

Craft, J.A., Gilbert, J.A., Temperton, B., Dempsey, K.E., Ashelford, K., Tiwari, B., Hutchinson, T.H., Chipman, J.K., 2010. Pyrosequencing of *Mytilus galloprovincialis* cDNAs: tissue-specific expression patterns. PLoS ONE 5, e8875.

Cummings, V., Hewitt, J., Van Rooyen, A., Currie, K., Beard, S., Thrush, S., Norkko, J., Barr, N., Heath, P., Halliday, N.J., 2011. Ocean acidification at high latitudes: Potential effects on functioning of the Antarctic bivalve *Laternula elliptica*. PloS one 6, e16069.

de Wit, P., Palumbi, S.R., 2013. Transcriptome-wide polymorphisms of red abalone (*Haliotis rufescens*) reveal patterns of gene flow and local adaptation. Molecular Ecology 22, 2884-2897.
Dickson, A.G., 1990. Thermodynamics of the dissociation of boric acid in synthetic seawater from 273.15 to 318.15 K. Deep Sea Research Part A. Oceanographic Research Papers 37, 755-766.
Dickson, A.G., Millero, F.J., 1987. A comparison of the equilibrium constants for the dissociation of carbonic acid in seawater media. Deep Sea Research Part A. Oceanographic Research Papers 34, 1733-1743.
du Plessis, L., Skunca, N., Dessimoz, C., 2011. The what, where, how and why of gene ontology - a primer for bioinformaticians. Briefings in bioinformatics 12, 723-735.
Edgar, R.C., 2004. MUSCLE: multiple sequence alignment with high accuracy and high throughput. Nucleic acids research 32, 1792-1797.
Ekblom, R., Galindo, J., 2011. Applications of next generation sequencing in molecular ecology of non-model organisms. Heredity 107, 1-15.
Evans, T.G., Chan, F., Menge, B.A., Hofmann, G.E., 2013. Transcriptomic responses to ocean acidification in larval sea urchins from a naturally variable pH environment. Molecular Ecology 22, 1609-1625.
Fabry, V.J., Seibel, B.A., Feely, R.A., Orr, J.C., 2008. Impacts of ocean acidification on marine fauna and ecosystem processes. ICES Journal of Marine Science 65, 414–432.
Fiedler, T.J., Hudder, A., McKay, S.J., Shivkumar, S., Capo, T.R., Schmale, M.C., Walsh, P.J., 2010. The transcriptome of the early life history stages of the California Sea Hare *Aplysia californica*. Comparative biochemistry and physiology. Part D, Genomics & proteomics 5, 165-170.
Franchini, P., Van der Merwe, M., Roodt-Wilding, R., 2011. Transcriptome characterization of the South African abalone *Haliotis midae* using sequencing-by-synthesis. BMC research notes 4, 59.
Freer, A., Bridgett, S., Jiang, J., Cusack, M., 2014. Biomineral proteins from *Mytilus edulis* mantle tissue transcriptome. Marine Biotechnology 16, 34-45.
Gardner, L., Mills, D., Wiegand, A., Leavesley, D., Elizur, A., 2011. Spatial analysis of biomineralization associated gene expression from the mantle organ of the pearl oyster *Pinctada maxima*. BMC genomics 12, 455.
Gattuso, J.P., Allemand, D., Frankignoulle, M., 1999. Photosynthesis and calcification at cellular, organismal and community levels in coral reefs: A review on interactions and control by carbonate chemistry. Integrative and Comparative Biology 39, 160-183.
Gayral, P., Weinert, L., Chiari, Y., Tsagkogeorga, G., Ballenghien, M., Galtier, N., 2011. Next-generation sequencing of transcriptomes: a guide to RNA isolation in nonmodel animals. Molecular Ecology Resources 11, 650-661.
Grabherr, M.G., Haas, B.J., Yassour, M., Levin, J.Z., Thompson, D.A., Amit, I., Adiconis, X., Fan, L., Raychowdhury, R., Zeng, Q., 2011. Full-length transcriptome assembly from RNA-Seq data without a reference genome. Nature biotechnology 29, 644-652.
Haas, B.J., Papanicolaou, A., Yassour, M., Grabherr, M., Blood, P.D., Bowden, J., Couger, M.B., Eccles, D., Li, B., Lieber, M., 2013. *De novo* transcript sequence reconstruction from RNA-seq using the Trinity platform for reference generation and analysis. Nature Protocols 8, 1494-1512.

Harms, L., Frickenhaus, S., Schiffer, M., Mark, F.C., Storch, D., Pörtner, H.-O., Held, C., Lucassen, M., 2013. Characterization and analysis of a transcriptome from the boreal spider crab *Hyas araneus*. Comparative Biochemistry and Physiology Part D: Genomics and Proteomics 8, 344-351.

Hendriks, I.E., Duarte, C.M., Álvarez, M., 2010. Vulnerability of marine biodiversity to ocean acidification: A meta-analysis. Estuarine, Coastal and Shelf Science 86, 157-164.

Heyland, A., Vue, Z., Voolstra, C.R., Medina, M., Moroz, L.L., 2011. Developmental transcriptome of *Aplysia californica*. Journal of Experimental Zoology Part B: Molecular and Developmental Evolution 316, 113-134.

Howes, E.L., Bednaršek, N., Büdenbender, J., Comeau, S., Doubleday, A., Gallager, S.M., Hopcroft, R.R., Lischka, S., Maas, A.E., Bijma, J., 2014. Sink and swim: a status review of thecosome pteropod culture techniques. Journal of Plankton Research 36, 299-315.

Huang, X., Zhao, M., Liu, W., Guan, Y., Shi, Y., Wang, Q., Wu, S., He, M., 2012. Gigabase-Scale Transcriptome Analysis on Four Species of Pearl Oysters. Marine Biotechnology doi: 10.1007/s10126-10012-19484-x.

Hüning, A.K., Melzner, F., Thomsen, J., Gutowska, M.A., Krämer, L., Frickenhaus, S., Rosenstiel, P., Pörtner, H.-O., Philipp, E.E., Lucassen, M., 2012. Impacts of seawater acidification on mantle gene expression patterns of the Baltic Sea blue mussel: implications for shell formation and energy metabolism. Marine Biology, 1-17.

Hüning, A.K., Melzner, F., Thomsen, J., Gutowska, M.A., Krämer, L., Frickenhaus, S., Rosenstiel, P., Pörtner, H.-O., Philipp, E.E., Lucassen, M., 2013. Impacts of seawater acidification on mantle gene expression patterns of the Baltic Sea blue mussel: implications for shell formation and energy metabolism. Marine Biology 160, 1845-1861.

Hunt, B.P.V., Pakhomov, E.A., Hosie, G.W., Siegel, V., Ward, P., Bernard, K., 2008. Pteropods in Southern Ocean ecosystems. Progress in Oceanography 78, 193-221.

Hunter, S., Jones, P., Mitchell, A., Apweiler, R., Attwood, T.K., Bateman, A., Bernard, T., Binns, D., Bork, P., Burge, S., 2011. InterPro in 2011: new developments in the family and domain prediction database. Nucleic Acids Research, gkr948.

I.P.C.C., 2007. Climate Change 2007: The Physical Science Basis. Contribution of Working Group I to the Fourth Assessment Report of the Intergovernmental Panel on Climate Change, in: S. Solomon, D. Qin, M. Manning, Z. Chen, M. Marquis, K.B. Averyt, M. Tignor, H.L. Miller (Eds.). Cambridge Univ Press, Cambridge, UK.

Iobst, S.T., Drickamer, K., 1994. Binding of sugar ligands to Ca (2+)-dependent animal lectins. II. Generation of high-affinity galactose binding by site-directed mutagenesis. Journal of Biological Chemistry 269, 15512-15519.

Jackson, D.J., Macis, L., Reitner, J., Degnan, B.M., Wörheide, G., 2007. Sponge paleogenomics reveals an ancient role for carbonic anhydrase in skeletogenesis. Science 316, 1893-1895.

Jackson, D.J., McDougall, C., Woodcroft, B., Moase, P., Rose, R.A., Kube, M., Reinhardt, R., Rokhsar, D.S., Montagnani, C., Joubert, C., 2010. Parallel evolution of nacre building gene sets in molluscs. Molecular biology and evolution 27, 591-608.

Joubert, C., Piquemal, D., Marie, B., Manchon, L., Pierrat, F., Zanella-Cléon, I., Cochennec-Laureau, N., Gueguen, Y., Montagnani, C., 2010. Transcriptome and proteome analysis of *Pinctada margaritifera* calcifying mantle and shell: focus on biomineralization. BMC genomics 11, 613.

Kaniewska, P., Campbell, P.R., Kline, D.I., Rodriguez-Lanetty, M., Miller, D.J., Dove, S., Hoegh-Guldberg, O., 2012. Major Cellular and Physiological Impacts of Ocean Acidification on a Reef Building Coral. PLoS ONE 7, e34659.

Kroeker, K.J., Kordas, R.L., Crim, R., Hendriks, I.E., Ramajo, L., Singh, G.S., Duarte, C.M., Gattuso, J.P., 2013. Impacts of ocean acidification on marine organisms: quantifying sensitivities and interaction with warming. Global change biology 19, 1884-1896.

Kroeker, K.J., Kordas, R.L., Crim, R.N., Singh, G.G., 2010. Meta-analysis reveals negative yet variable effects of ocean acidification on marine organisms. Ecology Letters 13, 1419-1434.

Kurihara, H., Takano, Y., Kurokawa, D., Akasaka, K., 2012. Ocean acidification reduces biomineralization-related gene expression in the sea urchin, *Hemicentrotus pulcherrimus*. Marine Biology 159, 2819-2826.

Lalli, C.M., Gilmer, R.W., 1989. Pelagic Snails: The Biology of Holoplanktonic Gastropod Mollusks. Stanford University Press, Stanford, CA.

Langenbuch, M., Pörtner, H.O., 2004. High sensitivity to chronically elevated CO_2 levels in a eurybathic marine sipunculid. Aquatic Toxicology 70, 55-61.

Langmead, B., Trapnell, C., Pop, M., Salzberg, S.L., 2009. Ultrafast and memory-efficient alignment of short DNA sequences to the human genome. Genome Biol 10, R25.

Lin, J.-Y., Ma, K.-Y., Bai, Z.-Y., Li, J.-L., 2013. Molecular cloning and characterization of perlucin from the freshwater pearl mussel, *Hyriopsis cumingii*. Gene 526, 210-216.

Lischka, S., Riebesell, U., 2012. Synergistic effects of ocean acidification and warming on overwintering pteropods in the Arctic. Global Change Biology 18, 3517-3528.

Liu, W., Huang, X., Lin, J., He, M., 2012. Seawater acidification and elevated temperature affect gene expression patterns of the pearl oyster *Pinctada fucata*. PLoS ONE 7, e33679.

Lohse, M., Bolger, A.M., Nagel, A., Fernie, A.R., Lunn, J.E., Stitt, M., Usadel, B., 2012. RobiNA: A user-friendly, integrated software solution for RNA-Seq-based transcriptomics. Nucleic Acids Research 40, W622-W627.

Maas, A.E., Wang, Z.A., Lawson, G.L., in review. The metabolic response of thecosome pteropods from the North Atlantic and North Pacific Oceans to high CO_2 and low O_2. Limnology and Oceanography.

Maas, A.E., Wishner, K.F., Seibel, B.A., 2012. The metabolic response of pteropods to acidification reflects natural CO_2-exposure in oxygen minimum zones. Biogeosciences 9, 747-757.

Mann, K., Weiss, I.M., Andre, S., Gabius, H.J., Fritz, M., 2000. The amino-acid sequence of the abalone (*Haliotis laevigata*) nacre protein perlucin. European Journal of Biochemistry 267, 5257-5264.

Manno, C., Morata, N., Primicerio, R., 2012. *Limacina retroversa*'s response to combined effects of ocean acidification and sea water freshening. Estuarine, Coastal and Shelf Science 113, 163–171.

Manno, C., Tirelli, V., Accornero, A., Fonda Umani, S., 2010. Importance of the contribution of *Limacina helicina* faecal pellets to the carbon pump in Terra Nova Bay (Antarctica). Journal of Plankton Research 32, 145-152.

Marsh, A.G., Manahan, D.T., 1999. A method for accurate measurements of the respiration rates of marine invertebrate embryos and larvae. Marine Ecology Progress Series 184, 1-10.

Mehrbach, C., Culberson, C., Hawley, J., Pytkowicz, R., 1973. Measurement of the apparent dissociation constants of carbonic acid in seawater at atmospheric pressure. Limnology and Oceanography 18, 897-907.

Melzner, F., Thomsen, J., Koeve, W., Oschlies, A., Gutowska, M.A., Bange, H.W., Hansen, H.P., Körtzinger, A., 2013. Future ocean acidification will be amplified by hypoxia in coastal habitats. Marine Biology 160, 1875-1888.

Meyer, E., Aglyamova, G., Matz, M., 2011. Profiling gene expression responses of coral larvae (*Acropora millepora*) to elevated temperature and settlement inducers using a novel RNA-Seq procedure. Molecular Ecology 20, 3599-3616.

Miles, H., Widdicombe, S., Spicer, J.I., Hall-Spencer, J., 2007. Effects of anthropogenic seawater acidification on acid–base balance in the sea urchin *Psammechinus miliaris*. Marine Pollution Bulletin 54, 89-96.

Moya, A., Huisman, L., Ball, E., Hayward, D., Grasso, L., Chua, C., Woo, H., Gattuso, J.P., Forêt, S., Miller, D., 2012. Whole transcriptome analysis of the coral *Acropora millepora* reveals complex responses to CO_2 driven acidification during the initiation of calcification. Molecular Ecology.

Moya, A., Tambutté, S., Bertucci, A., Tambutté, E., Lotto, S., Vullo, D., Supuran, C.T., Allemand, D., Zoccola, D., 2008. Carbonic anhydrase in the scleractinian coral *Stylophora pistillata*. Journal of Biological Chemistry 283, 25475-25484.

Mu, C., Song, X., Zhao, J., Wang, L., Qiu, L., Zhang, H., Zhou, Z., Wang, M., Song, L., Wang, C., 2012. A scallop C-type lectin from *Argopecten irradians* (AiCTL5) with activities of lipopolysaccharide binding and Gram-negative bacteria agglutination. Fish & Shellfish Immunology 32, 716-723.

O'Donnell, M.J., Todgham, A.E., Sewell, M.A., Hammond, L.T.M., Ruggiero, K., Fangue, N.A., Zippay, M.L., Hofmann, G.E., 2010. Ocean acidification alters skeletogenesis and gene expression in larval sea urchins. Marine Ecology Progress Series 398, 157-171.

Picone, B., Rhode, C., Roodt-Wilding, R., 2015. Transcriptome profiles of wild and cultured South African abalone, *Haliotis midae*. Marine Genomics 20, 3-6.

Pierrot, D., Lewis, E., Wallace, D., 2006. Co2sys DOS Program developed for CO_2 system calculations. Carbon Dioxide Information Analysis Center, Oak Ridge National Laboratory, US Department of Energy. ORNL/CDIAC-105. .

Riebesell, U., Fabry, V.J., Hansson, L., Gattuso, J.P., 2010. Guide to best practices for ocean acidification research and data reporting. Publications Office of the European Union.

Riebesell, U., Zondervan, I., Rost, B., Tortell, P.D., Zeebe, R.E., Morel, F.M.M., 2000. Reduced calcification of marine plankton in response to increased atmospheric CO_2. Nature 407, 364-367.

Robinson, M.D., McCarthy, D.J., Smyth, G.K., 2010. edgeR: a Bioconductor package for differential expression analysis of digital gene expression data. Bioinformatics 26, 139-140.

Robinson, M.D., Oshlack, A., 2010. A scaling normalization method for differential expression analysis of RNA-seq data. Genome Biol 11, R25.

Sadamoto, H., Takahashi, H., Okada, T., Kenmoku, H., Toyota, M., Asakawa, Y., 2012. De novo sequencing and transcriptome analysis of the central nervous system of mollusc *Lymnaea stagnalis* by deep RNA sequencing. PLoS ONE 7, e42546.

Seibel, B.A., Fabry, V.J., 2003. Marine biotic response to elevated carbon dioxide. Advances in Applied Biodiversity Science 4, 59-67.

Seibel, B.A., Maas, A.E., Dierssen, H.M., 2012. Energetic plasticity underlies a variable response to ocean acidification in the pteropod, *Limacina helicina antarctica.* . PLoS ONE 7, e30464.

Seibel, B.A., Walsh, P.J., 2001. Potential impacts of CO_2 injection on deep-sea biota. Science 294, 319-320.
Shi, Y., Yu, C., Gu, Z., Zhan, X., Wang, Y., Wang, A., 2012. Characterization of the pearl oyster (*Pinctada martensii*) mantle transcriptome unravels biomineralization genes. Marine Biotechnology, doi:10.1007/s10126-10012-19476-x.
Sleight, V.A., Thorne, M.A., Peck, L.S., Clark, M.S., 2015. Transcriptomic response to shell damage in the Antarctic clam, *Laternula elliptica*: Time scales and spatial localisation. Marine genomics 20, 45-55.
Stumpp, M., Dupont, S., Thorndyke, M., Melzner, F., 2011a. CO_2 induced seawater acidification impacts sea urchin larval development II: Gene expression patterns in pluteus larvae. Comparative Biochemistry and Physiology-Part A: Molecular & Integrative Physiology 160, 320-330.
Stumpp, M., Trübenbach, K., Brennecke, D., Hu, M., Melzner, F., 2012. Resource allocation and extracellular acid–base status in the sea urchin *Strongylocentrotus droebachiensis* in response to CO_2 induced seawater acidification. Aquatic Toxicology 110, 194-207.
Stumpp, M., Wren, J., Melzner, F., Thorndyke, M., Dupont, S., 2011b. CO_2 induced seawater acidification impacts sea urchin larval development I: Elevated metabolic rates decrease scope for growth and induce developmental delay. Comparative Biochemistry and Physiology-Part A: Molecular & Integrative Physiology 160, 331-340.
Todgham, A.E., Hofmann, G.E., 2009. Transcriptomic response of sea urchin larvae *Strongylocentrotus purpuratus* to CO_2-driven seawater acidification. Journal of Experimental Biology 212, 2579-2594.
Venier, P., Varotto, L., Rosani, U., Millino, C., Celegato, B., Bernante, F., Lanfranchi, G., Novoa, B., Roch, P., Figueras, A., 2011. Insights into the innate immunity of the Mediterranean mussel *Mytilus galloprovincialis*. BMC genomics 12, 69.
Vijay, N., Poelstra, J.W., Künstner, A., Wolf, J.B.W., 2012. Challenges and strategies in transcriptome assembly and differential gene expression quantification. A comprehensive in silico assessment of RNA-seq experiments. Molecular Ecology, online preprint.
Wang, L., Feng, Z., Wang, X., Wang, X., Zhang, X., 2010. DEGseq: an R package for identifying differentially expressed genes from RNA-seq data. Bioinformatics 26, 136-138.
Wang, N., Lee, Y.-H., Lee, J., 2008. Recombinant perlucin nucleates the growth of calcium carbonate crystals: Molecular cloning and characterization of perlucin from disk abalone, *Haliotis discus discus*. Comparative Biochemistry and Physiology Part B: Biochemistry and Molecular Biology 149, 354-361.
Wang, Z.A., Bienvenu, D.J., Mann, P.J., Hoering, K.A., Poulsen, J.R., Spencer, R.G., Holmes, R.M., 2013a. Inorganic carbon speciation and fluxes in the Congo River. Geophys Res Lett 40, 511-516.
Wang, Z.A., Cai, W.-J., 2004. Carbon dioxide degassing and inorganic carbon export from a marsh-dominated estuary (the Duplin River): A marsh CO_2 pump. Limnology and Oceanography 49, 341-354.
Wang, Z.A., Wanninkhof, R., Cai, W.J., Byrne, R.H., Hu, X., Peng, T.H., Huang, W.J., 2013b. The marine inorganic carbon system along the Gulf of Mexico and Atlantic Coasts of the United States: Insights from a transregional coastal carbon study. Limnol. Oceanogr. 58, 325-342.

Weiss, I.M., Kaufmann, S., Mann, K., Fritz, M., 2000. Purification and characterization of perlucin and perlustrin, two new proteins from the shell of the mollusc *Haliotis laevigata*. Biochemical and biophysical research communications 267, 17-21.

Winnebeck, E.C., Millar, C.D., Warman, G.R., 2010. Why does insect RNA look degraded? Journal of Insect Science 10, 1-7.

Xie, L.-p., Zhu, F.-j., Zhou, Y.-j., Yang, C., Zhang, R.-q., 2011. Molecular Approaches to Understand Biomineralization of Shell Nacreous Layer. Molecular Biomineralization, 331-352.

Yang, J., Wang, L., Zhang, H., Qiu, L., Wang, H., Song, L., 2011. C-type lectin in *Chlamys farreri* (CfLec-1) mediating immune recognition and opsonization. PLoS ONE 6, e17089.

Zeng, V., Villanueva, K.E., Ewen-Campen, B.S., Alwes, F., Browne, W.E., Extavour, C.G., 2011. De novo assembly and characterization of a maternal and developmental transcriptome for the emerging model crustacean *Parhyale hawaiensis*. BMC genomics 12, 581.

Zhang, C., Zhang, R., 2006. Matrix proteins in the outer shells of molluscs. Marine Biotechnology 8, 572-586.

Zhang, G., Fang, X., Guo, X., Li, L., Luo, R., Xu, F., Yang, P., Zhang, L., Wang, X., Qi, H., 2012. The oyster genome reveals stress adaptation and complexity of shell formation. Nature 490, 49-54.

Zhao, X., Wang, Q., Jiao, Y., Huang, R., Deng, Y., Wang, H., Du, X., 2012a. Identification of genes potentially related to biomineralization and immunity by transcriptome analysis of pearl sac in pearl oyster *Pinctada martensii*. Marine Biotechnology 14, 730-739.

Zhao, X., Yu, H., Kong, L., Li, Q., 2012b. Transcriptomic responses to salinity stress in the Pacific oyster *Crassostrea gigas*. PLoS ONE 7, e46244.

Zippay, M.K.L., Hofmann, G.E., 2010. Effect of pH on gene expression and thermal tolerance of early life history stages of red abalone (*Haliotis rufescens*). Journal of Shellfish Research 29, 429-439.

Figure Legends:

Figure 1: Oxygen consumption rates (µmol g^{-1} h^{-1}) of the individual pteropods used in the transcriptomic study that were exposed to ambient CO_2 (~380 ppm, dark red circles) and high CO_2 (~800 ppm, dark blue circles). There was no significant difference between the treatments even when the dataset was expanded to include more individuals from the Atlantic (light colored circles) and individuals from the Pacific (light colored diamonds) (datapoints from Maas et al., in review).

Figure 2: Heat map comparing the gene expression patterns among eight individual pteropods. Depicts a Bray-Curtis similarity matrix of the standardized edgeR normalized (TMM, trimmed mean of M-values; Robinson and Oshlack, 2010) fragments per kilobase per million reads mapped (FPKM) transcript counts for all genes that were expressed in at least two of the eight study individuals. Letters A-D correspond to individuals exposed to high CO_2, and letters E-H correspond to individuals exposed to ambient CO_2; analysis constructed without grouping individuals by treatment.

Figure 3: Alignment of the conserved domain of the C-type lectin domain family proteins. The six highly conserved cysteine residues are labeled with stars, open circles label the residues putatively involved in calcium-dependent carbohydrate binding (Mann et al., 2000) and grey boxes contain the motifs proposed to determine carbohydrate-binding specificity for galactose (Iobst and Drickamer, 1994). Amino acid residue that consist of over 75% of the sequences are documented as identical (dark grey shading) or similar (light grey shading) overlaying the sequence.

Tables:

Table 1: The carbonate chemistry parameters for the experiments including temperature (T.) salinity (S.), and measured dissolved inorganic carbon (DIC). These were used, along with the manufacturer's certification of the gas concentration (ppm calculation), to calculate the aragonite saturation state (Ω_{Ar}) and pH of the treatments using CO2SYS. The calculations were also made incorporating one standard deviation away from the nominal gas concentration (± 2%) to characterize the certainty of the treatment (ppm calculation ± 2%), as well as by using the measured TA of the batch of water (2307.3; TA calculation, grey box). The TA measurements are likely not representative of conditions during the actual experiments as a consequence of ongoing biological activity in the batch of water between the point at which it was sampled for TA and when it was used for respiration experiments (see text). Irrespective of the choice of parameters, the calculations resulted in similar estimates of the pH and Ω_{Ar} and suggest that the two treatments were distinctly different.

				ppm calculation		ppm calculation ± 2%			TA calculation		
Treatment	T.	S.	DIC ± SD								
	°C	psu	(µmol kg^{-1})	Ω_{Ar}	pH	pCO_2 (µatm)	Ω_{Ar}	pH	pCO_2 (µatm)	Ω_{Ar}	pH
380 ppm	15	33	2036.3 ± 57.9	2.44	8.06	372.4 - 387.6	2.49 - 2.40	8.07 - 8.05	350.6	2.66	8.10
800 ppm	15	33	2194.9 ± 19.9	1.41	7.78	797.2 - 829.7	1.43 - 1.38	7.77 - 7.79	830.1	1.38	7.77

Table 2: Transcripts that were identified as differentially expressed ($p < 0.05$) in the full dataset are listed with their putative annotation via BLASTX against the nr database (BLASTX ID) along with GO annotation, the e-value and percent similarity (% sim.) of the transcript to the top match. Also reported is the log base 2 fold change (Log FC), log counts per million (Log CPM) and the false discovery rate (FDR) of the analysis reported by edgeR.

Transcript ID	BLASTX ID	e-value	% sim.	Log FC	Log CPM	FDR	GO Annotation
GAWL01006673	cytochrome c oxidase subunit iii	1.90E-13	76.9	-10.34	9.88	0.010	P:aerobic electron transport chain; C:integral to membrane; C:mitochondrion; F:cytochrome-c oxidase activity
GAWL01040808	cytochrome c oxidase subunit i	2.40E-22	87.8	-10.04	9.25	0.010	P:aerobic respiration; C:mitochondrial inner membrane; C:respiratory chain; F:electron carrier activity; F:iron ion binding; P:oxidative phosphorylation; F:heme binding; C:integral to membrane; P:electron transport chain; F:cytochrome-c oxidase activity
GAWL01040684	venom allergen 5-like	2.60E-23	53.8	7.07	2.27	0.040	F:hydrolase activity; C:extracellular region
GAWL01040977	lactose-binding lectin l-2-like, BAA19861.1 (perlucin)	5.70E-14	51.0	7.27	1.31	0.041	F:carbohydrate binding
GAWL01006926	transcription factor glial cells missing	9.90E-60	69.1	7.62	1.23	0.035	P:regulation of transcription, DNA-dependent; F:DNA binding
GAWL01040816	conglutinin 1	2.10E-08	46.9	8.80	0.12	0.040	F:carbohydrate binding
GAWL01040704	chymotrypsin-like elastase family member 1-like	7.80E-13	52.1	11.08	0.25	0.008	P:single-organism process; P:regulation of cellular process; F:serine-type endopeptidase activity; P:proteolysis
GAWL01040711	polycystic kidney disease protein 1-like 2-like	6.30E-06	54.8	11.29	0.38	0.040	F:protein binding

926

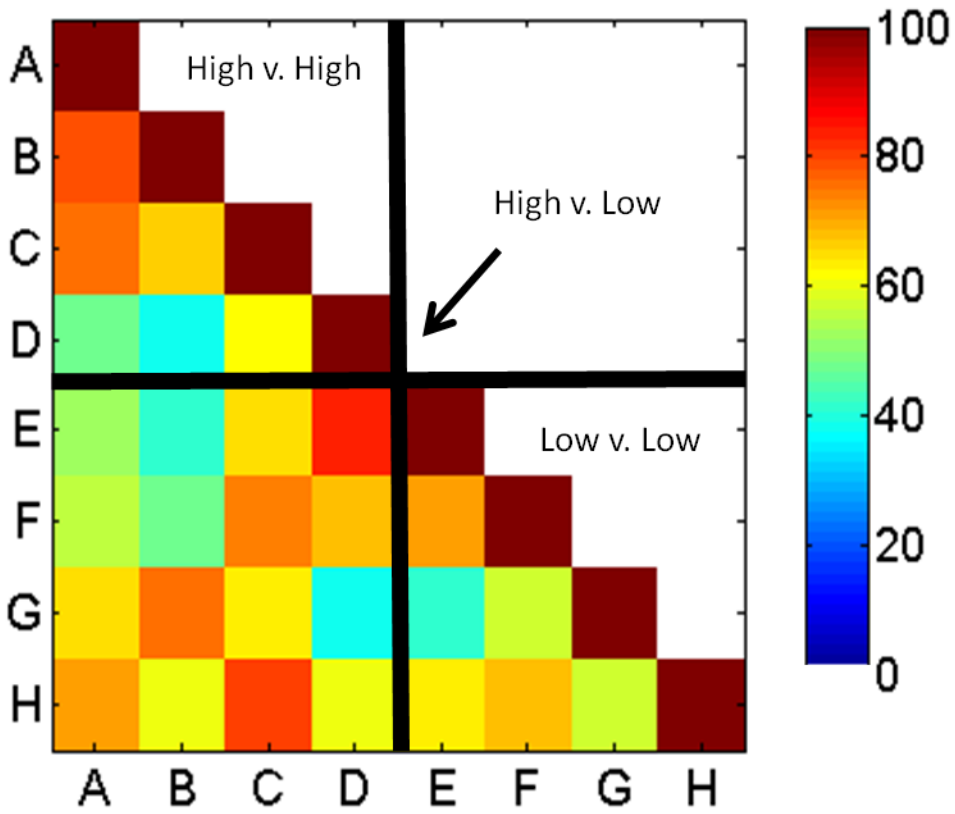
High v. High
High v. Low
Low v. Low
A
B
C
D
E
F
G
H
A B C D E F G H
100
80
60
40
20
0

927

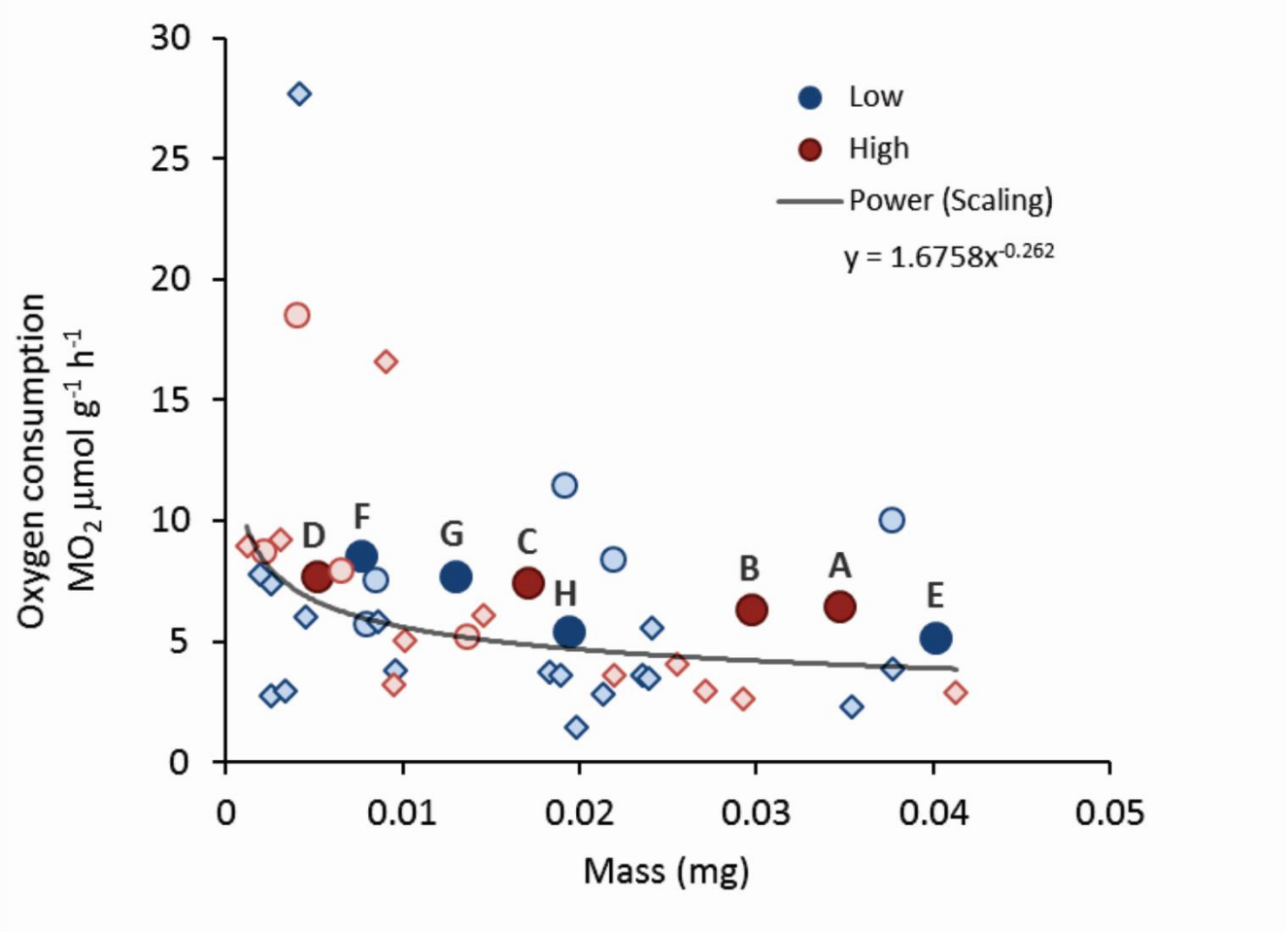
Low
High
Power (Scaling)
y = 1.6758x-0.262
Oxygen consumption
MO2 µmol g-1 h-1
Mass (mg)
0
5
10
15
20
25
30
0
0.01
0.02
0.03
0.04
0.05
D
F
G
C
H
B
A
E

928

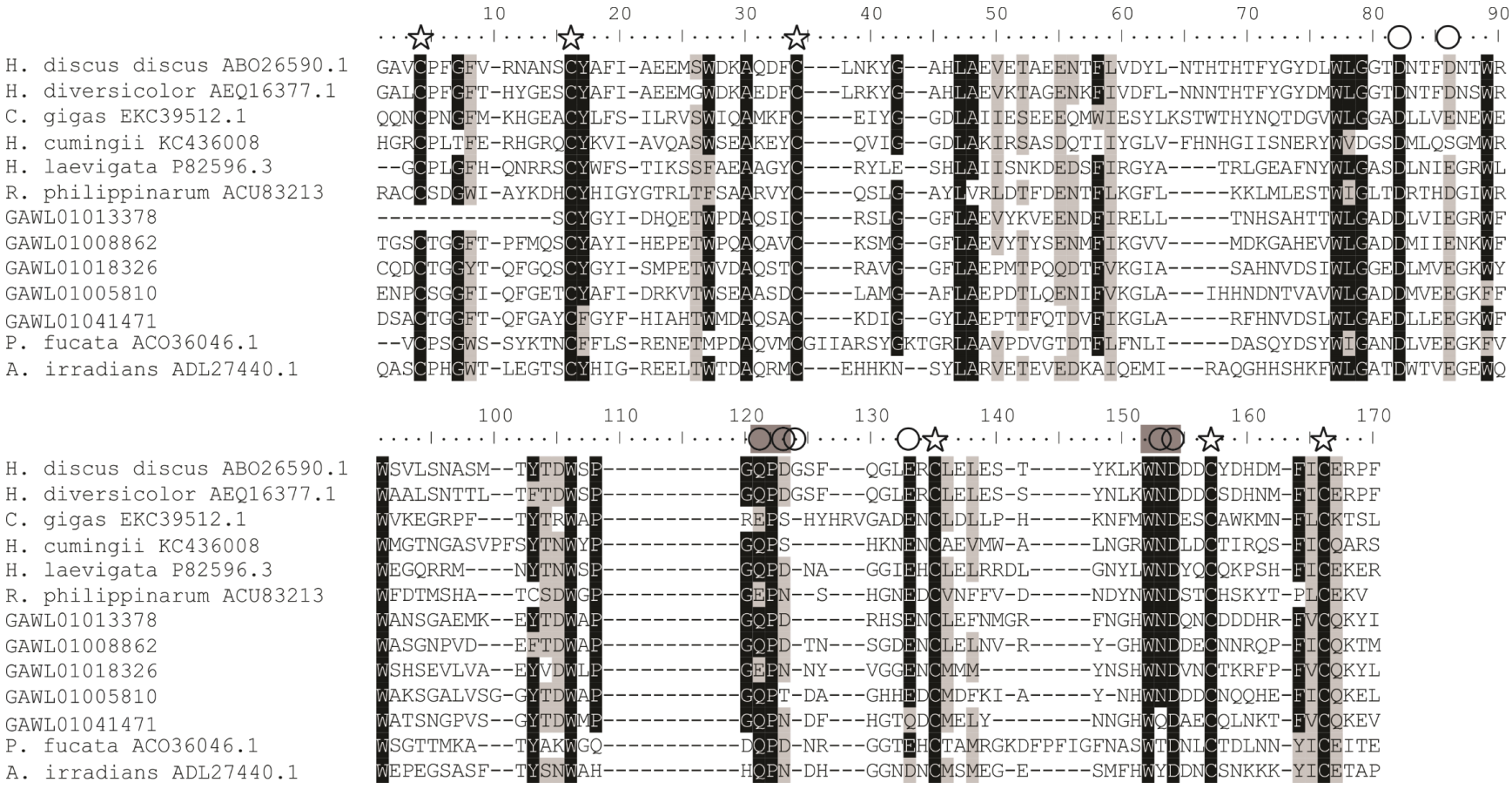
10 20 30 40 50 60 70 80 90
H. discus discus ABO26590.1 GAVCPFGFV-RNANSCYAFI-AEEMSWDKAQDFC---LNKYG--AHLAEVETAEENTFLVDYL-NTHTHTFYGYDLWLGTDNTFDNTWR
H. diversicolor AEQ16377.1 GALCPFGFT-HYGESCYAFI-AEEMGWDKAEDFC---LRKYG--AHLAEVKTAGENKFIVDFL-NNNTHTFYGYDMWLGTDNTFDNSWR
C. gigas EKC39512.1 QQNCPNGFM-KHGEACYLFS-ILRVSWIQAMKFC----EIYG--GDLAIIESEEEQMWIESYLKSTWTHYNQTDGVWLGGADLLVENEWE
H. cumingii KC436008 HGRCPLTFE-RHGRQCYKVI-AVQASWSEAKEYC----QVIG--GDLAKIRSASDQTIIYGLV-FHNHGIISNERYWVDGSDMLQSGMWR
H. laevigata P82596.3 --GCPLGFH-QNRRSCYWFS-TIKSSFAEAAGYC----RYLE--SHLAIISNKDEDSFIRGYA----TRLGEAFNYWLGASDLNIEGRWL
R. philippinarum ACU83213 RACCSDGWI-AYKDHCYHIGYGTRLTFSAARVYC----QSLG--AYLVRLDTFDENTFLKGFL-----KKLMLESTWIGLTDRTHDGIWR
GAWL01013378 ----------SCYGYI-DHQETWPDAQSIC----RSLG--GFLAEVYKVEENDFIRELL-----TNHSAHTTWLGADDLVIEGRWF
GAWL01008862 TGSCTGGFT-PFMQSCYAYI-HEPETWPQAQAVC----KSMG--GFLAEVYTYSENMFIKGVV-----MDKGAHEVWLGADDMIIENKWF
GAWL01018326 CQDCTGGYT-QFGQSCYGYI-SMPETWVDAQSTC----RAVG--GFLAEPMTPQQDTFVKGIA-----SAHNVDSIWLGGEDLMVEGKWY
GAWL01005810 ENPCSGGFI-QFGETCYAFI-DRKVTWSEAASDC----LAMG--AFLAEPDTLQENIFVKGLA---IHHNDNTVAVWLGADDMVEEGKFF
GAWL01041471 DSACTGGFT-QFGAYCFGYF-HIAHTWMDAQSAC----KDIG--GYLAEPTTFQTDVFIKGLA-----RFHNVDSLWLGAEDLLEEGKWF
P. fucata ACO36046.1 --VCPSGWS-SYKTNCFFLS-RENETMPDAQVMCGIIARSYGKTGRLAAVPDVGTDTFLFNLI-----DASQYDSYWIGANDLVEEGKFV
A. irradians ADL27440.1 QASCPHGWT-LEGTSCYHIG-REELTWTDAQRMC---EHHKN--SYLARVETEVEDKAIQEMI---RAQGHHSHKFWLGATDWTVEGEWQ
100 110 120 130 140 150 160 170
H. discus discus ABO26590.1 WSVLSNASM--TYTDWSP----------GQPDGSF---QGLERCLELES-T-----YKLKWNDDDCYDHDM-FICERPF
H. diversicolor AEQ16377.1 WAALSNTTL--TFTDWSP----------GQPDGSF---QGLERCLELES-S-----YNLKWNDDDCSDHNM-FICERPF
C. gigas EKC39512.1 WVKEGRPF---TYTRWAP----------REPS-HYHRVGADENCLDLLP-H-----KNFMWNDESCAWKMN-FLCKTSL
H. cumingii KC436008 WMGTNGASVPFSYTNWYP----------GQPS------HKNENCAEVMW-A-----LNGRWNDLDCTIRQS-FICQARS
H. laevigata P82596.3 WEGQRRM----NYTNWSP----------GQPD-NA---GGIEHCLELRRDL-----GNYLWNDYQCQKPSH-FICEKER
R. philippinarum ACU83213 WFDTMSHA---TCSDWGP----------GEPN--S---HGNEDCVNFFV-D-----NDYNWNDSTCHSKYT-PLCEKV
GAWL01013378 WANSGAEMK--EYTDWAP----------GQPD------RHSENCLEFNMGR-----FNGHWNDQNCDDDHR-FVCQKYI
GAWL01008862 WASGNPVD---EFTDWAP----------GQPD-TN---SGDENCLELNV-R-----Y-GHWNDDECNNRQP-FICQKTM
GAWL01018326 WSHSEVLVA--EYVDWLP----------GEPN-NY---VGGENCMMM---------YNSHWNDVNCTKRFP-FVCQKYL
GAWL01005810 WAKSGALVSG-GYTDWAP----------GQPT-DA---GHHEDCMDFKI-A-----Y-NHWNDDDCNQQHE-FICQKEL
GAWL01041471 WATSNGPVS--GYTDWMP----------GQPN-DF---HGTQDCMELY--------NNGHWQDAECQLNKT-FVCQKEV
P. fucata ACO36046.1 WSGTTMKA---TYAKWGQ----------DQPD-NR---GGTEHCTAMRGKDFPFIGFNASWTDNLCTDLNN-YICEITE
A. irradians ADL27440.1 WEPEGSASF--TYSNWAH----------HQPN-DH---GGNDNCMSMEG-E-----SMFHWYDDNCSNKKK-YICETAP

929

Supplementary File 1:

The experiments were conducted as part of a larger multi-species and multi-region study (Maas et al., submitted). The Reeve tow from which the animals used in this transcriptomics analysis were collected was conducted on 8/21/11 at 21:16 local time, was 20 minutes in duration and was made with 200 m of wire out (~150 m depth). Hydrographic parameters of the water column were taken from a CTD made at the same station on the same day (Figure S1).

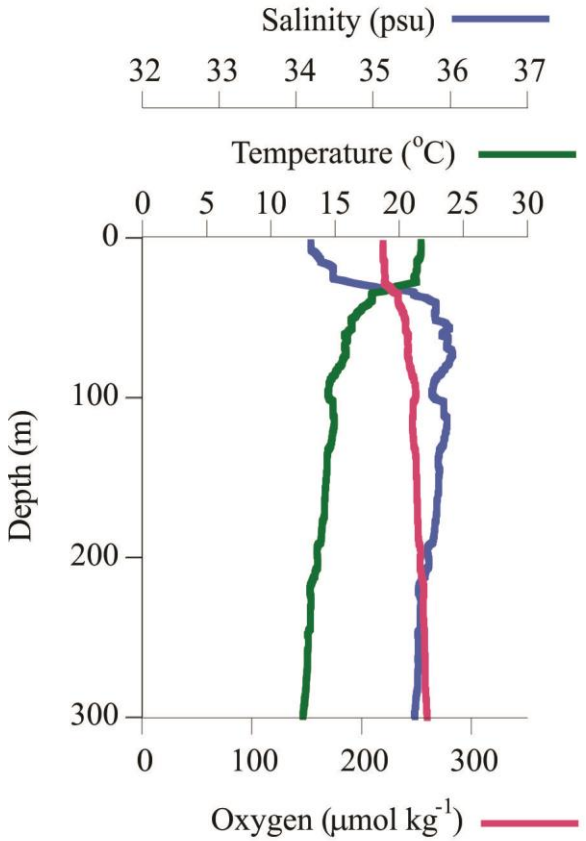

Figure S1: Hydrographic parameters from the site of *C. pyramidata* collection taken with a CTD.

Full dataset for respiration experiments available at BCO-DMO
Handle: http://hdl.handle.net/1912/6421
DOI: 10.1575/1912/6421

Maas, A.E., Wang, Z.A., Lawson, G.L., submitted. The metabolic response of thecosome pteropods from the North Atlantic and North Pacific Oceans to high CO_2 and low O_2. Limnology and Oceanography.

Supplementary File 2: Candidate sequences (Transcript ID) with a putative involvement in biomineralization were identified by TBLASTN with an e-value cutoff of <1.0 e^{-6} against sequences from other known molluscan biomineralization genes or sequences that were highly expressed in the *Crassostrea gigas* mantle (Zhang *et al.*, 2012). The Genbank accession number (Molluscan Match) is reported for each identification (BLAST).

Zhang G, Fang X, Guo X, et al. (2012) The oyster genome reveals stress adaptation and complexity of shell formation. Nature 490, 49-54

Transcript ID	Molluscan Match	BLAST	length (bp)	# hits	min. e-value	similarity mean
GAWL01002040	ABO10190.1	67kd laminin receptor precursor	1159	1	4.50E-127	80.00%
GAWL01007520	AAO83853.1	af484096_1calcium calmodulin-dependent serine protein kinase 1	352	2	1.20E-09	51.00%
GAWL01008523	AAO83853.1	af484096_1calcium calmodulin-dependent serine protein kinase 1	201	1	5.20E-09	59.00%
GAWL01008525	AAO83853.1	af484096_1calcium calmodulin-dependent serine protein kinase 1	233	2	3.30E-12	57.50%
GAWL01008839	AAO83853.1	af484096_1calcium calmodulin-dependent serine protein kinase 1	959	1	2.30E-07	45.00%
GAWL01009550	AAO83853.1	af484096_1calcium calmodulin-dependent serine protein kinase 1	313	2	4.00E-08	47.50%
GAWL01010250	AAO83853.1	af484096_1calcium calmodulin-dependent serine protein kinase 1	481	1	5.00E-10	48.00%
GAWL01012098	AAO83853.1	af484096_1calcium calmodulin-dependent serine protein kinase 1	688	2	1.20E-15	56.00%
GAWL01012491	AAO83853.1	af484096_1calcium calmodulin-dependent serine protein kinase 1	697	2	1.90E-14	43.50%
GAWL01012519	AAO83853.1	af484096_1calcium calmodulin-dependent serine protein kinase 1	1316	2	3.60E-13	46.50%
GAWL01014498	AAO83853.1	af484096_1calcium calmodulin-dependent serine protein kinase 1	2426	2	1.00E-41	48.50%
GAWL01020303	AAO83853.1	af484096_1calcium calmodulin-dependent serine protein kinase 1	1466	2	1.90E-17	43.00%
GAWL01022326	AAO83853.1	af484096_1calcium calmodulin-dependent serine protein kinase 1	1794	1	3.20E-19	47.00%
GAWL01022800	AAO83853.1	af484096_1calcium calmodulin-dependent serine protein kinase 1	1724	3	2.00E-15	48.33%

GAWL01029840	AAO83853.1	af484096_1calcium calmodulin-dependent serine protein kinase 1	2010	2	2.10E-19	43.50%
GAWL01029841	AAO83853.1	af484096_1calcium calmodulin-dependent serine protein kinase 1	3422	2	5.70E-19	43.50%
GAWL01030131	AAO83853.1	af484096_1calcium calmodulin-dependent serine protein kinase 1	1853	2	1.30E-13	40.50%
GAWL01031237	AAO83853.1	af484096_1calcium calmodulin-dependent serine protein kinase 1	1837	2	1.30E-12	44.50%
GAWL01031239	AAO83853.1	af484096_1calcium calmodulin-dependent serine protein kinase 1	1771	2	1.20E-12	44.50%
GAWL01041551	AAO83853.1	af484096_1calcium calmodulin-dependent serine protein kinase 1	1537	1	1.00E-07	44.00%
GAWL01042634	AAO83853.1	af484096_1calcium calmodulin-dependent serine protein kinase 1	638	2	2.20E-11	41.50%
GAWL01043425	AAO83853.1	af484096_1calcium calmodulin-dependent serine protein kinase 1	341	2	7.80E-11	53.50%
GAWL01001168	AAO83853.1	af484096_1calcium calmodulin-dependent serine protein kinase 1	1134	3	1.70E-16	43.00%
GAWL01001865	AAO83853.1	af484096_1calcium calmodulin-dependent serine protein kinase 1	1961	2	3.80E-08	51.00%
GAWL01002231	AAO83853.1	af484096_1calcium calmodulin-dependent serine protein kinase 1	1455	2	9.00E-21	44.50%
GAWL01002699	AAO83853.1	af484096_1calcium calmodulin-dependent serine protein kinase 1	913	2	8.10E-12	47.50%
GAWL01004308	AAO83853.1	af484096_1calcium calmodulin-dependent serine protein kinase 1	420	2	2.40E-07	48.00%
GAWL01006046	AAV69062.1	alkaline phosphatase	243	1	1.20E-20	68.00%
GAWL01007068	AAV69062.1	alkaline phosphatase	228	1	3.30E-11	62.00%
GAWL01021034	AAV69062.1	alkaline phosphatase	955	1	4.10E-51	68.00%
GAWL01018085	ABF13208.1	amorphous calcium carbonate binding protein 1	1414	1	1.30E-11	43.00%
GAWL01019754	ABF13208.1	amorphous calcium carbonate binding protein 1	1051	1	1.70E-10	45.00%
GAWL01021558	ABF13208.1	amorphous calcium carbonate binding protein 1	307	1	3.80E-08	47.00%
GAWL01022734	ABF13208.1	amorphous calcium carbonate binding protein 1	1561	1	1.30E-08	41.00%
GAWL01023481	ABF13208.1	amorphous calcium carbonate binding protein 1	1273	1	4.30E-13	40.00%
GAWL01028996	ABF13208.1	amorphous calcium carbonate binding protein 1	776	1	1.70E-20	45.00%

GAWL01036492	ABF13208.1	amorphous calcium carbonate binding protein 1	1557	1	1.60E-10	37.00%
GAWL01037328	ABF13208.1	amorphous calcium carbonate binding protein 1	876	1	5.80E-21	47.00%
GAWL01037329	ABF13208.1	amorphous calcium carbonate binding protein 1	865	1	4.40E-21	47.00%
GAWL01016209	AAQ63463.1	BMSP	617	2	4.30E-09	48.50%
GAWL01005835	BAK86420.1	BMSP	1237	1	3.20E-17	48.00%
GAWL01007088	BAK86420.1	BMSP	266	1	3.10E-12	60.00%
GAWL01007170	BAK86420.1	BMSP	1139	1	2.60E-15	45.00%
GAWL01007692	BAK86420.1	BMSP	306	1	6.40E-08	61.00%
GAWL01009973	BAK86420.1	BMSP	635	1	8.20E-11	53.00%
GAWL01011067	BAK86420.1	BMSP	1210	2	2.90E-33	44.50%
GAWL01011767	BAK86420.1	BMSP	1392	1	4.00E-08	44.00%
GAWL01012090	BAK86420.1	BMSP	350	1	7.30E-07	52.00%
GAWL01016206	BAK86420.1	BMSP	1163	1	3.40E-15	43.00%
GAWL01018515	BAK86420.1	BMSP	2154	2	7.30E-20	46.00%
GAWL01018538	BAK86420.1	BMSP	2099	1	6.50E-29	43.00%
GAWL01019168	BAK86420.1	BMSP	1780	2	1.00E-07	46.50%
GAWL01019169	BAK86420.1	BMSP	1831	2	1.10E-07	46.50%
GAWL01021256	BAK86420.1	BMSP	1554	1	8.60E-12	48.00%
GAWL01021777	BAK86420.1	BMSP	1054	1	3.80E-11	49.00%
GAWL01021778	BAK86420.1	BMSP	963	1	5.50E-07	47.00%
GAWL01023192	BAK86420.1	BMSP	353	1	8.80E-09	47.00%
GAWL01023193	BAK86420.1	BMSP	341	1	3.00E-11	50.00%
GAWL01023911	BAK86420.1	BMSP	1342	2	2.10E-16	39.00%
GAWL01024166	BAK86420.1	BMSP	912	1	5.00E-30	45.00%
GAWL01024167	BAK86420.1	BMSP	840	1	1.00E-29	45.00%
GAWL01024373	BAK86420.1	BMSP	836	1	2.20E-19	54.00%
GAWL01024795	BAK86420.1	BMSP	1739	1	8.10E-19	54.00%
GAWL01024796	BAK86420.1	BMSP	1783	1	8.60E-19	54.00%
GAWL01026614	BAK86420.1	BMSP	968	1	1.80E-07	45.00%

GAWL01027077	BAK86420.1	BMSP	645	1	7.80E-09	60.00%
GAWL01027487	BAK86420.1	BMSP	391	1	1.30E-09	52.00%
GAWL01027568	BAK86420.1	BMSP	2341	1	2.10E-09	45.00%
GAWL01027593	BAK86420.1	BMSP	953	1	3.20E-17	48.00%
GAWL01027594	BAK86420.1	BMSP	902	1	2.90E-17	48.00%
GAWL01027595	BAK86420.1	BMSP	977	1	3.60E-17	48.00%
GAWL01027596	BAK86420.1	BMSP	744	1	1.70E-17	48.00%
GAWL01028835	BAK86420.1	BMSP	1121	1	5.30E-08	41.00%
GAWL01028836	BAK86420.1	BMSP	1109	1	5.30E-08	41.00%
GAWL01029398	BAK86420.1	BMSP	3047	2	2.40E-71	43.00%
GAWL01029399	BAK86420.1	BMSP	3003	2	2.80E-71	43.00%
GAWL01029400	BAK86420.1	BMSP	549	1	8.40E-22	54.00%
GAWL01029531	BAK86420.1	BMSP	1859	1	6.20E-20	43.00%
GAWL01029612	BAK86420.1	BMSP	1649	1	1.40E-20	50.00%
GAWL01029613	BAK86420.1	BMSP	1722	1	1.60E-20	50.00%
GAWL01029935	BAK86420.1	BMSP	1935	1	1.70E-22	46.00%
GAWL01030751	BAK86420.1	BMSP	2672	1	1.10E-14	50.00%
GAWL01032487	BAK86420.1	BMSP	556	1	2.50E-08	59.00%
GAWL01032488	BAK86420.1	BMSP	1836	1	2.00E-28	45.00%
GAWL01032490	BAK86420.1	BMSP	1955	1	7.20E-22	40.00%
GAWL01032730	BAK86420.1	BMSP	1341	1	2.10E-09	55.00%
GAWL01040474	BAK86420.1	BMSP	1021	1	1.70E-21	49.00%
GAWL01040934	BAK86420.1	BMSP	1580	2	1.70E-33	44.50%
GAWL01044612	BAK86420.1	BMSP	452	1	6.30E-10	49.00%
GAWL01006819	ACI96106.1	calcineurin a subunit	1242	1	1.20E-64	59.00%
GAWL01002013	ACI96106.1	calcineurin a subunit	2175	1	3.50E-65	63.00%
GAWL01003543	ACI96106.1	calcineurin a subunit	611	1	2.40E-82	93.00%
GAWL01003544	ACI96106.1	calcineurin a subunit	339	1	3.90E-83	99.00%
GAWL01011445	ACI96107.1	calcineurin b subunit	726	1	1.10E-08	47.00%

GAWL01022964	ACI96107.1	calcineurin b subunit	913	2	1.30E-09	50.50%
GAWL01030364	ACI96107.1	calcineurin b subunit	1408	1	1.10E-07	52.00%
GAWL01038612	ACI96107.1	calcineurin b subunit	821	1	1.20E-10	49.00%
GAWL01038613	ACI96107.1	calcineurin b subunit	593	1	4.20E-11	49.00%
GAWL01005846	AAU93878.1	calcium-dependent protein kinase	919	1	2.10E-26	61.00%
GAWL01024944	AAU93878.1	calcium-dependent protein kinase	679	1	5.40E-08	49.00%
GAWL01025644	AAU93878.1	calcium-dependent protein kinase	239	1	2.20E-07	64.00%
GAWL01004991	AAU93878.1	calcium-dependent protein kinase	941	4	1.40E-17	45.50%
GAWL01022742	AAQ20043.1	calmodulin	1276	2	1.60E-11	49.00%
GAWL01008433	ACI22622.1	calmodulin	236	2	7.80E-07	54.00%
GAWL01014244	ACI22622.1	calmodulin	231	2	8.70E-10	53.00%
GAWL01014561	ACI22622.1	calmodulin	306	2	8.70E-15	94.00%
GAWL01024577	ACI22622.1	calmodulin	435	2	1.90E-07	55.50%
GAWL01011531	AAQ20043.1	calmodulin-like protein	5590	3	3.90E-12	54.67%
GAWL01013700	AAQ20043.1	calmodulin-like protein	540	4	6.20E-32	60.25%
GAWL01014562	AAQ20043.1	calmodulin-like protein	335	6	1.30E-63	71.50%
GAWL01014655	AAQ20043.1	calmodulin-like protein	1710	3	1.70E-26	58.00%
GAWL01015148	AAQ20043.1	calmodulin-like protein	897	3	7.00E-24	51.67%
GAWL01017236	AAQ20043.1	calmodulin-like protein	1500	3	5.60E-31	61.67%
GAWL01023182	AAQ20043.1	calmodulin-like protein	1017	3	5.60E-23	58.33%
GAWL01023184	AAQ20043.1	calmodulin-like protein	1273	4	6.20E-24	55.75%
GAWL01023185	AAQ20043.1	calmodulin-like protein	1293	4	6.80E-24	56.00%
GAWL01023919	AAQ20043.1	calmodulin-like protein	1897	4	1.90E-27	68.25%
GAWL01025368	AAQ20043.1	calmodulin-like protein	766	3	1.30E-22	54.00%
GAWL01025369	AAQ20043.1	calmodulin-like protein	738	3	9.90E-23	54.00%
GAWL01025370	AAQ20043.1	calmodulin-like protein	999	3	1.50E-22	54.00%
GAWL01026783	AAQ20043.1	calmodulin-like protein	1722	3	8.00E-34	65.00%
GAWL01034793	AAQ20043.1	calmodulin-like protein	830	4	3.60E-13	50.50%
GAWL01034794	AAQ20043.1	calmodulin-like protein	776	4	2.70E-13	50.50%

GAWL01041627	AAQ20043.1	calmodulin-like protein	937	5	3.60E-38	61.80%
GAWL01002706	AAQ20043.1	calmodulin-like protein	644	4	2.50E-12	48.75%
GAWL01004554	AAQ20043.1	calmodulin-like protein	685	3	3.10E-26	62.33%
GAWL01012421	AAV73912.1	calmodulin-like protein	1427	4	3.20E-09	59.00%
GAWL01017805	AAV73912.1	calmodulin-like protein	2042	1	3.20E-11	55.00%
GAWL01045336	AAV73912.1	calmodulin-like protein	250	3	1.60E-08	50.00%
GAWL01005925	ACI22622.1	calmodulin-like protein	745	3	5.50E-26	58.33%
GAWL01006019	ACI22622.1	calmodulin-like protein	293	4	1.80E-16	67.00%
GAWL01007472	ACI22622.1	calmodulin-like protein	649	4	4.10E-26	62.00%
GAWL01009136	ACI22622.1	calmodulin-like protein	734	4	1.80E-53	65.00%
GAWL01009322	ACI22622.1	calmodulin-like protein	708	3	1.80E-08	45.67%
GAWL01014441	ACI22622.1	calmodulin-like protein	633	3	4.60E-16	50.67%
GAWL01018034	ACI22622.1	calmodulin-like protein	736	4	3.90E-45	66.75%
GAWL01018851	ACI22622.1	calmodulin-like protein	860	5	6.00E-39	61.00%
GAWL01019614	ACI22622.1	calmodulin-like protein	655	3	3.30E-12	47.67%
GAWL01019615	ACI22622.1	calmodulin-like protein	772	3	5.60E-12	47.00%
GAWL01019780	ACI22622.1	calmodulin-like protein	1222	3	6.70E-24	57.67%
GAWL01019781	ACI22622.1	calmodulin-like protein	643	3	2.10E-26	58.67%
GAWL01019782	ACI22622.1	calmodulin-like protein	1249	3	2.20E-25	58.67%
GAWL01019783	ACI22622.1	calmodulin-like protein	1222	3	5.90E-24	57.67%
GAWL01019784	ACI22622.1	calmodulin-like protein	616	3	6.20E-25	57.67%
GAWL01019785	ACI22622.1	calmodulin-like protein	616	3	5.50E-25	57.67%
GAWL01022582	ACI22622.1	calmodulin-like protein	917	3	7.30E-28	63.00%
GAWL01025672	ACI22622.1	calmodulin-like protein	1063	4	3.40E-21	52.50%
GAWL01025673	ACI22622.1	calmodulin-like protein	623	4	8.00E-22	52.50%
GAWL01025754	ACI22622.1	calmodulin-like protein	1075	6	4.00E-100	72.33%
GAWL01025755	ACI22622.1	calmodulin-like protein	968	6	1.20E-100	72.33%
GAWL01025756	ACI22622.1	calmodulin-like protein	1043	6	2.80E-100	72.33%
GAWL01025757	ACI22622.1	calmodulin-like protein	1112	6	8.10E-101	72.33%

GAWL01025758	ACI22622.1	calmodulin-like protein	1005	6	2.40E-101	72.33%
GAWL01025759	ACI22622.1	calmodulin-like protein	1080	6	5.60E-101	72.33%
GAWL01032739	ACI22622.1	calmodulin-like protein	1349	3	9.50E-27	59.67%
GAWL01032740	ACI22622.1	calmodulin-like protein	2042	3	5.30E-26	59.67%
GAWL01032742	ACI22622.1	calmodulin-like protein	695	3	3.50E-28	60.33%
GAWL01033371	ACI22622.1	calmodulin-like protein	1319	3	2.30E-21	54.67%
GAWL01033372	ACI22622.1	calmodulin-like protein	916	3	4.60E-22	54.67%
GAWL01040509	ACI22622.1	calmodulin-like protein	2132	6	3.80E-98	72.17%
GAWL01001403	ACI22622.1	calmodulin-like protein	245	3	1.60E-09	68.67%
GAWL01040477	ABR68546.1	calreticulin	1807	1	1.40E-178	87.00%
GAWL01006317	AAX16122.1	carbonic anhydrase precursor	372	8	6.60E-14	55.00%
GAWL01014728	AAX16122.1	carbonic anhydrase precursor	501	8	1.10E-41	49.50%
GAWL01025152	AAX16122.1	carbonic anhydrase precursor	1322	8	2.50E-50	45.75%
GAWL01025154	AAX16122.1	carbonic anhydrase precursor	1370	8	6.40E-30	44.25%
GAWL01030114	AAX16122.1	carbonic anhydrase precursor	571	8	1.30E-13	52.13%
GAWL01030115	AAX16122.1	carbonic anhydrase precursor	1145	8	1.10E-12	52.25%
GAWL01030119	AAX16122.1	carbonic anhydrase precursor	966	8	6.60E-13	52.25%
GAWL01030121	AAX16122.1	carbonic anhydrase precursor	591	8	1.20E-13	52.13%
GAWL01036321	AAX16122.1	carbonic anhydrase precursor	1252	8	7.10E-38	58.00%
GAWL01041171	AAX16122.1	carbonic anhydrase precursor	502	2	3.50E-17	53.00%
GAWL01043375	AAX16122.1	carbonic anhydrase precursor	267	2	2.60E-11	56.00%
GAWL01011206	BAJ52887.1	carbonic anhydrase-related protein viii	845	8	3.60E-53	48.50%
GAWL01030123	BAJ52887.1	carbonic anhydrase-related protein viii	715	8	8.90E-14	53.13%
GAWL01021323	AAY86556.1	chitin synthase	6849	2	2.70E-17	43.50%
GAWL01040313	AAY86556.1	chitin synthase	939	2	7.30E-47	61.00%
GAWL01040314	AAY86556.1	chitin synthase	638	2	8.10E-39	56.00%
GAWL01040294	AAY86556.1	chitin synthase	1047	2	4.20E-43	47.50%
GAWL01040301	BAF73720.1	chitin synthase	2448	2	1.30E-50	44.50%
GAWL01040302	BAF73720.1	chitin synthase	2786	2	3.30E-50	44.50%

GAWL01040310	BAF73720.1	chitin synthase	1561	2	9.40E-47	47.00%
GAWL01040311	BAF73720.1	chitin synthase	2377	2	3.90E-45	47.00%
GAWL01040312	BAF73720.1	chitin synthase	1755	2	3.80E-53	43.50%
GAWL01040318	BAF73720.1	chitin synthase	2039	2	1.60E-45	47.00%
GAWL01006661	ACO36045.1	c-type lectin 1	770	1	7.90E-07	52.00%
GAWL01006662	ACO36045.1	c-type lectin 1	730	1	7.10E-07	52.00%
GAWL01008024	ACO36045.1	c-type lectin 1	1032	2	6.60E-12	43.00%
GAWL01008710	ACO36045.1	c-type lectin 1	432	1	9.20E-11	55.00%
GAWL01015091	ACO36045.1	c-type lectin 1	1157	6	3.80E-14	44.17%
GAWL01015921	ACO36045.1	c-type lectin 1	276	2	1.20E-09	51.00%
GAWL01021731	ACO36045.1	c-type lectin 1	2114	1	1.20E-08	39.00%
GAWL01023945	ACO36045.1	c-type lectin 1	210	1	3.70E-14	60.00%
GAWL01024711	ACO36045.1	c-type lectin 1	1360	1	9.20E-08	46.00%
GAWL01026387	ACO36045.1	c-type lectin 1	3322	3	6.20E-13	43.67%
GAWL01030133	ACO36045.1	c-type lectin 1	300	2	1.20E-07	46.50%
GAWL01033405	ACO36045.1	c-type lectin 1	545	6	1.10E-11	49.67%
GAWL01033407	ACO36045.1	c-type lectin 1	580	6	2.10E-11	49.67%
GAWL01038897	ACO36045.1	c-type lectin 1	1192	1	7.60E-07	48.00%
GAWL01038905	ACO36045.1	c-type lectin 1	643	1	4.00E-07	48.00%
GAWL01039996	ACO36045.1	c-type lectin 1	999	1	3.70E-08	53.00%
GAWL01040010	ACO36045.1	c-type lectin 1	287	2	6.30E-09	49.00%
GAWL01040002	ACO36045.1	c-type lectin 1	887	1	3.00E-08	53.00%
GAWL01040664	ACO36045.1	c-type lectin 1	662	1	5.40E-16	49.00%
GAWL01041666	ACO36045.1	c-type lectin 1	531	1	6.10E-09	49.00%
GAWL01043724	ACO36045.1	c-type lectin 1	563	2	2.20E-12	47.50%
GAWL01044548	ACO36045.1	c-type lectin 1	542	1	1.80E-09	41.00%
GAWL01023942	ADD16957.1	c-type lectin 1	736	5	4.20E-15	43.20%
GAWL01006345	ACO36046.1	c-type lectin 2	243	3	6.20E-10	51.33%
GAWL01008852	ACO36046.1	c-type lectin 2	492	3	5.00E-10	45.33%

GAWL01011796	ACO36046.1	c-type lectin 2	324	2	4.90E-07	50.50%
GAWL01013902	ACO36046.1	c-type lectin 2	475	2	1.60E-12	45.00%
GAWL01016430	ACO36046.1	c-type lectin 2	630	1	3.90E-08	38.00%
GAWL01018912	ACO36046.1	c-type lectin 2	398	2	1.20E-09	50.50%
GAWL01018913	ACO36046.1	c-type lectin 2	439	2	1.10E-09	49.00%
GAWL01023929	ACO36046.1	c-type lectin 2	1029	2	3.90E-10	44.50%
GAWL01028413	ACO36046.1	c-type lectin 2	896	8	2.00E-16	49.38%
GAWL01028415	ACO36046.1	c-type lectin 2	860	8	1.80E-16	49.38%
GAWL01030072	ACO36046.1	c-type lectin 2	947	2	1.60E-08	41.50%
GAWL01034777	ACO36046.1	c-type lectin 2	432	2	2.90E-08	48.00%
GAWL01037099	ACO36046.1	c-type lectin 2	556	1	2.90E-08	42.00%
GAWL01044073	ACO36046.1	c-type lectin 2	251	1	4.80E-07	47.00%
GAWL01005427	ABO26644.1	derm_biogl ame: full=dermatopontin ame: full=tyrosine-rich acidic matrix protein short=tramp	647	2	9.70E-22	50.00%
GAWL01006549	ABO26644.1	derm_biogl ame: full=dermatopontin ame: full=tyrosine-rich acidic matrix protein short=tramp	751	2	5.00E-25	48.50%
GAWL01007316	ABO26644.1	derm_biogl ame: full=dermatopontin ame: full=tyrosine-rich acidic matrix protein short=tramp	396	2	8.20E-09	55.50%
GAWL01011602	ABO26644.1	derm_biogl ame: full=dermatopontin ame: full=tyrosine-rich acidic matrix protein short=tramp	748	2	6.60E-13	46.50%
GAWL01012778	ABO26644.1	derm_biogl ame: full=dermatopontin ame: full=tyrosine-rich acidic matrix protein short=tramp	559	2	1.70E-11	56.50%
GAWL01013075	ABO26644.1	derm_biogl ame: full=dermatopontin ame: full=tyrosine-rich acidic matrix protein short=tramp	648	2	3.30E-34	52.50%
GAWL01016999	ABO26644.1	derm_biogl ame: full=dermatopontin ame: full=tyrosine-rich acidic matrix protein short=tramp	678	2	5.00E-34	51.50%
GAWL01018852	ABO26644.1	derm_biogl ame: full=dermatopontin ame: full=tyrosine-rich acidic matrix protein short=tramp	775	2	3.40E-11	58.00%
GAWL01018853	ABO26644.1	derm_biogl ame: full=dermatopontin ame: full=tyrosine-rich acidic matrix protein short=tramp	826	2	4.10E-11	58.00%
GAWL01020398	ABO26644.1	derm_biogl ame: full=dermatopontin ame: full=tyrosine-rich acidic matrix protein short=tramp	676	2	5.30E-24	46.50%
GAWL01022052	ABO26644.1	derm_biogl ame: full=dermatopontin ame: full=tyrosine-rich acidic matrix protein short=tramp	657	2	2.70E-29	49.50%

GAWL01026459	ABO26644.1	derm_biogl ame: full=dermatopontin ame: full=tyrosine-rich acidic matrix protein short=tramp	1333	2	8.80E-20	56.50%
GAWL01033187	ABO26644.1	derm_biogl ame: full=dermatopontin ame: full=tyrosine-rich acidic matrix protein short=tramp	452	2	8.70E-24	58.50%
GAWL01033189	ABO26644.1	derm_biogl ame: full=dermatopontin ame: full=tyrosine-rich acidic matrix protein short=tramp	458	2	9.70E-24	58.50%
GAWL01033190	ABO26644.1	derm_biogl ame: full=dermatopontin ame: full=tyrosine-rich acidic matrix protein short=tramp	1279	2	9.50E-20	61.00%
GAWL01033191	ABO26644.1	derm_biogl ame: full=dermatopontin ame: full=tyrosine-rich acidic matrix protein short=tramp	1242	2	8.50E-20	61.00%
GAWL01040568	ABO26644.1	derm_biogl ame: full=dermatopontin ame: full=tyrosine-rich acidic matrix protein short=tramp	561	2	9.70E-12	51.00%
GAWL01001212	ABO26644.1	derm_biogl ame: full=dermatopontin ame: full=tyrosine-rich acidic matrix protein short=tramp	452	2	4.00E-31	53.50%
GAWL01002418	ABO26644.1	derm_biogl ame: full=dermatopontin ame: full=tyrosine-rich acidic matrix protein short=tramp	689	2	3.60E-22	48.00%
GAWL01009495	P83553.1	derm_biogl ame: full=dermatopontin ame: full=tyrosine-rich acidic matrix protein short=tramp	357	2	1.30E-18	57.50%
GAWL01016131	P83553.1	derm_biogl ame: full=dermatopontin ame: full=tyrosine-rich acidic matrix protein short=tramp	366	2	1.40E-16	55.50%
GAWL01017752	P83553.1	derm_biogl ame: full=dermatopontin ame: full=tyrosine-rich acidic matrix protein short=tramp	783	1	7.60E-07	53.00%
GAWL01017753	P83553.1	derm_biogl ame: full=dermatopontin ame: full=tyrosine-rich acidic matrix protein short=tramp	771	1	7.50E-07	53.00%
GAWL01019808	P83553.1	derm_biogl ame: full=dermatopontin ame: full=tyrosine-rich acidic matrix protein short=tramp	757	2	1.60E-33	53.50%
GAWL01021600	P83553.1	derm_biogl ame: full=dermatopontin ame: full=tyrosine-rich acidic matrix protein short=tramp	694	1	1.50E-08	60.00%
GAWL01024781	P83553.1	derm_biogl ame: full=dermatopontin ame: full=tyrosine-rich acidic matrix protein short=tramp	1110	1	4.90E-08	55.00%
GAWL01024782	P83553.1	derm_biogl ame: full=dermatopontin ame: full=tyrosine-rich acidic matrix protein short=tramp	1187	1	5.30E-08	55.00%
GAWL01034338	P83553.1	derm_biogl ame: full=dermatopontin ame: full=tyrosine-rich acidic matrix protein short=tramp	730	2	3.90E-32	52.50%
GAWL01041264	P83553.1	derm_biogl ame: full=dermatopontin ame: full=tyrosine-rich acidic matrix protein short=tramp	339	1	9.30E-10	63.00%
GAWL01001213	P83553.1	derm_biogl ame: full=dermatopontin ame: full=tyrosine-rich acidic matrix protein short=tramp	302	2	2.60E-09	58.50%

GAWL01001346	P83553.1	derm_biogl ame: full=dermatopontin ame: full=tyrosine-rich acidic matrix protein short=tramp	277	2	1.00E-09	57.50%
GAWL01026575	ABO26644.1	dermatopontin	2342	1	2.90E-08	67.00%
GAWL01026577	ABO26644.1	dermatopontin	2449	1	3.10E-08	67.00%
GAWL01029650	ABO26644.1	dermatopontin	789	1	2.50E-08	62.00%
GAWL01029651	ABO26644.1	dermatopontin	2740	1	1.20E-07	62.00%
GAWL01033188	ABO26644.1	dermatopontin	397	1	8.80E-08	58.00%
GAWL01005477	AAQ63463.1	ep protein precursor	768	1	2.80E-13	55.00%
GAWL01006118	AAQ63463.1	ep protein precursor	456	1	1.00E-10	56.00%
GAWL01006208	AAQ63463.1	ep protein precursor	561	1	2.70E-11	47.00%
GAWL01007529	AAQ63463.1	ep protein precursor	991	1	6.80E-09	45.00%
GAWL01008640	AAQ63463.1	ep protein precursor	329	1	6.80E-08	50.00%
GAWL01009297	AAQ63463.1	ep protein precursor	399	1	2.20E-07	47.00%
GAWL01009403	AAQ63463.1	ep protein precursor	656	2	4.30E-16	45.50%
GAWL01010205	AAQ63463.1	ep protein precursor	448	2	2.10E-08	48.00%
GAWL01014391	AAQ63463.1	ep protein precursor	1021	1	3.80E-08	51.00%
GAWL01014590	AAQ63463.1	ep protein precursor	703	1	2.50E-08	42.00%
GAWL01015316	AAQ63463.1	ep protein precursor	421	1	6.10E-10	52.00%
GAWL01015660	AAQ63463.1	ep protein precursor	411	2	2.90E-13	50.00%
GAWL01015661	AAQ63463.1	ep protein precursor	395	2	3.10E-10	46.00%
GAWL01016805	AAQ63463.1	ep protein precursor	535	2	2.30E-10	48.00%
GAWL01016806	AAQ63463.1	ep protein precursor	522	2	1.10E-10	47.50%
GAWL01017973	AAQ63463.1	ep protein precursor	1128	1	5.00E-08	45.00%
GAWL01019476	AAQ63463.1	ep protein precursor	523	2	3.50E-10	48.50%
GAWL01019625	AAQ63463.1	ep protein precursor	407	1	1.40E-10	46.00%
GAWL01020125	AAQ63463.1	ep protein precursor	626	2	2.60E-08	47.00%
GAWL01020345	AAQ63463.1	ep protein precursor	977	1	4.10E-08	45.00%
GAWL01020877	AAQ63463.1	ep protein precursor	692	2	1.20E-07	47.00%
GAWL01021530	AAQ63463.1	ep protein precursor	609	2	1.30E-12	47.00%
GAWL01021543	AAQ63463.1	ep protein precursor	502	1	3.00E-07	48.00%

GAWL01021690	AAQ63463.1	ep protein precursor	531	2	5.40E-14	54.00%
GAWL01021993	AAQ63463.1	ep protein precursor	432	2	5.50E-11	46.50%
GAWL01021994	AAQ63463.1	ep protein precursor	448	2	7.90E-12	46.50%
GAWL01022422	AAQ63463.1	ep protein precursor	1146	2	2.40E-15	49.00%
GAWL01022457	AAQ63463.1	ep protein precursor	1167	2	7.00E-14	47.50%
GAWL01022513	AAQ63463.1	ep protein precursor	682	1	1.70E-10	41.00%
GAWL01022518	AAQ63463.1	ep protein precursor	800	1	5.60E-09	47.00%
GAWL01022649	AAQ63463.1	ep protein precursor	618	1	2.20E-10	53.00%
GAWL01022650	AAQ63463.1	ep protein precursor	660	1	2.80E-10	53.00%
GAWL01025037	AAQ63463.1	ep protein precursor	645	2	6.00E-08	42.50%
GAWL01025638	AAQ63463.1	ep protein precursor	422	2	6.40E-12	51.50%
GAWL01025630	AAQ63463.1	ep protein precursor	830	2	5.30E-16	44.50%
GAWL01025631	AAQ63463.1	ep protein precursor	645	2	1.20E-16	46.00%
GAWL01025635	AAQ63463.1	ep protein precursor	607	2	1.70E-11	49.50%
GAWL01025637	AAQ63463.1	ep protein precursor	422	1	1.10E-11	49.00%
GAWL01025714	AAQ63463.1	ep protein precursor	763	1	1.40E-09	46.00%
GAWL01025721	AAQ63463.1	ep protein precursor	857	1	1.80E-09	46.00%
GAWL01030734	AAQ63463.1	ep protein precursor	785	2	6.80E-10	45.00%
GAWL01030725	AAQ63463.1	ep protein precursor	849	2	2.50E-14	45.50%
GAWL01031677	AAQ63463.1	ep protein precursor	561	2	5.60E-10	53.00%
GAWL01031678	AAQ63463.1	ep protein precursor	1331	2	5.30E-09	53.00%
GAWL01032127	AAQ63463.1	ep protein precursor	402	1	3.50E-07	55.00%
GAWL01034030	AAQ63463.1	ep protein precursor	1064	2	1.10E-09	48.00%
GAWL01034031	AAQ63463.1	ep protein precursor	860	2	3.20E-09	47.00%
GAWL01035489	AAQ63463.1	ep protein precursor	1185	2	1.20E-14	44.00%
GAWL01035492	AAQ63463.1	ep protein precursor	1186	2	1.50E-14	48.00%
GAWL01035495	AAQ63463.1	ep protein precursor	1461	2	6.70E-10	45.50%
GAWL01035484	AAQ63463.1	ep protein precursor	1206	2	5.80E-14	48.00%
GAWL01035486	AAQ63463.1	ep protein precursor	1368	2	7.40E-14	47.50%

GAWL01038309	AAQ63463.1	ep protein precursor	488	2	7.10E-11	49.50%
GAWL01040758	AAQ63463.1	ep protein precursor	850	2	9.90E-15	47.50%
GAWL01040964	AAQ63463.1	ep protein precursor	662	2	5.50E-16	47.00%
GAWL01041273	AAQ63463.1	ep protein precursor	671	1	5.20E-13	44.00%
GAWL01041785	AAQ63463.1	ep protein precursor	371	2	2.30E-09	46.50%
GAWL01000795	AAQ63463.1	ep protein precursor	400	1	4.80E-08	49.00%
GAWL01000818	AAQ63463.1	ep protein precursor	361	2	6.30E-09	52.00%
GAWL01002287	AAQ63463.1	ep protein precursor	503	2	3.40E-12	47.50%
GAWL01002564	AAQ63463.1	ep protein precursor	765	1	1.30E-12	46.00%
GAWL01002565	AAQ63463.1	ep protein precursor	483	1	2.40E-07	55.00%
GAWL01003925	AAQ63463.1	ep protein precursor	468	2	6.50E-13	49.00%
GAWL01000494	BAK86420.1	ep protein precursor	256	1	2.80E-08	48.00%
GAWL01017133	P86734.1	epdr1_halai ame: full=ependymin-related protein 1 flags: precursor	972	1	2.50E-08	42.00%
GAWL01017134	P86734.1	epdr1_halai ame: full=ependymin-related protein 1 flags: precursor	1035	1	2.70E-08	42.00%
GAWL01016318	AAQ12076.1	ferritin-like protein	367	1	1.00E-11	64.00%
GAWL01022407	AAQ12076.1	ferritin-like protein	1108	1	4.20E-101	91.00%
GAWL01037867	AAQ12076.1	ferritin-like protein	902	1	2.20E-68	70.00%
GAWL01005727	Q5GIS3.1	gbb_pinfu ame: full=guanine nucleotide-binding protein subunit beta short=pfgbeta1 ame: full=g protein subunit beta-1	470	1	8.90E-63	98.00%
GAWL01005888	Q5GIS3.1	gbb_pinfu ame: full=guanine nucleotide-binding protein subunit beta short=pfgbeta1 ame: full=g protein subunit beta-1	775	1	8.30E-11	40.00%
GAWL01008644	Q5GIS3.1	gbb_pinfu ame: full=guanine nucleotide-binding protein subunit beta short=pfgbeta1 ame: full=g protein subunit beta-1	442	1	1.40E-07	42.00%
GAWL01008645	Q5GIS3.1	gbb_pinfu ame: full=guanine nucleotide-binding protein subunit beta short=pfgbeta1 ame: full=g protein subunit beta-1	312	1	2.10E-10	45.00%
GAWL01008849	Q5GIS3.1	gbb_pinfu ame: full=guanine nucleotide-binding protein subunit beta short=pfgbeta1 ame: full=g protein subunit	1322	1	9.70E-22	45.00%

		beta-1				
GAWL01011746	Q5GIS3.1	gbb_pinfu ame: full=guanine nucleotide-binding protein subunit beta short=pfgbeta1 ame: full=g protein subunit beta-1	1168	1	5.20E-10	37.00%
GAWL01011768	Q5GIS3.1	gbb_pinfu ame: full=guanine nucleotide-binding protein subunit beta short=pfgbeta1 ame: full=g protein subunit beta-1	354	1	5.80E-07	40.00%
GAWL01011945	Q5GIS3.1	gbb_pinfu ame: full=guanine nucleotide-binding protein subunit beta short=pfgbeta1 ame: full=g protein subunit beta-1	1619	1	8.60E-15	44.00%
GAWL01012560	Q5GIS3.1	gbb_pinfu ame: full=guanine nucleotide-binding protein subunit beta short=pfgbeta1 ame: full=g protein subunit beta-1	2248	1	6.50E-09	38.00%
GAWL01013576	Q5GIS3.1	gbb_pinfu ame: full=guanine nucleotide-binding protein subunit beta short=pfgbeta1 ame: full=g protein subunit beta-1	780	1	1.70E-07	44.00%
GAWL01000477	Q5GIS3.1	gbb_pinfu ame: full=guanine nucleotide-binding protein subunit beta short=pfgbeta1 ame: full=g protein subunit beta-1	441	1	5.70E-17	50.00%
GAWL01015422	Q5GIS3.1	gbb_pinfu ame: full=guanine nucleotide-binding protein subunit beta short=pfgbeta1 ame: full=g protein subunit beta-1	2546	1	4.00E-10	40.00%
GAWL01015738	Q5GIS3.1	gbb_pinfu ame: full=guanine nucleotide-binding protein subunit beta short=pfgbeta1 ame: full=g protein subunit beta-1	1077	1	6.00E-09	41.00%
GAWL01017139	Q5GIS3.1	gbb_pinfu ame: full=guanine nucleotide-binding protein subunit beta short=pfgbeta1 ame: full=g protein subunit beta-1	260	1	5.60E-08	47.00%
GAWL01017328	Q5GIS3.1	gbb_pinfu ame: full=guanine nucleotide-binding protein subunit beta short=pfgbeta1 ame: full=g protein subunit beta-1	1635	1	3.80E-07	45.00%
GAWL01019381	Q5GIS3.1	gbb_pinfu ame: full=guanine nucleotide-binding protein subunit beta short=pfgbeta1 ame: full=g protein subunit beta-1	1808	1	1.20E-10	59.00%
GAWL01019979	Q5GIS3.1	gbb_pinfu ame: full=guanine nucleotide-binding protein subunit beta short=pfgbeta1 ame: full=g protein subunit beta-1	1368	1	5.10E-11	40.00%

GAWL01021552	Q5GIS3.1	gbb_pinfu ame: full=guanine nucleotide-binding protein subunit beta short=pfgbeta1 ame: full=g protein subunit beta-1	879	1	2.50E-07	39.00%
GAWL01022312	Q5GIS3.1	gbb_pinfu ame: full=guanine nucleotide-binding protein subunit beta short=pfgbeta1 ame: full=g protein subunit beta-1	2005	1	1.40E-13	42.00%
GAWL01022313	Q5GIS3.1	gbb_pinfu ame: full=guanine nucleotide-binding protein subunit beta short=pfgbeta1 ame: full=g protein subunit beta-1	374	1	2.30E-07	43.00%
GAWL01022625	Q5GIS3.1	gbb_pinfu ame: full=guanine nucleotide-binding protein subunit beta short=pfgbeta1 ame: full=g protein subunit beta-1	1266	1	2.00E-11	43.00%
GAWL01022647	Q5GIS3.1	gbb_pinfu ame: full=guanine nucleotide-binding protein subunit beta short=pfgbeta1 ame: full=g protein subunit beta-1	1539	1	5.30E-10	41.00%
GAWL01024035	Q5GIS3.1	gbb_pinfu ame: full=guanine nucleotide-binding protein subunit beta short=pfgbeta1 ame: full=g protein subunit beta-1	1803	1	1.70E-18	46.00%
GAWL01024253	Q5GIS3.1	gbb_pinfu ame: full=guanine nucleotide-binding protein subunit beta short=pfgbeta1 ame: full=g protein subunit beta-1	1761	1	2.30E-14	38.00%
GAWL01024950	Q5GIS3.1	gbb_pinfu ame: full=guanine nucleotide-binding protein subunit beta short=pfgbeta1 ame: full=g protein subunit beta-1	1677	1	5.40E-16	43.00%
GAWL01025255	Q5GIS3.1	gbb_pinfu ame: full=guanine nucleotide-binding protein subunit beta short=pfgbeta1 ame: full=g protein subunit beta-1	1376	1	3.70E-12	40.00%
GAWL01027665	Q5GIS3.1	gbb_pinfu ame: full=guanine nucleotide-binding protein subunit beta short=pfgbeta1 ame: full=g protein subunit beta-1	1774	1	5.40E-14	38.00%
GAWL01027666	Q5GIS3.1	gbb_pinfu ame: full=guanine nucleotide-binding protein subunit beta short=pfgbeta1 ame: full=g protein subunit beta-1	573	1	3.30E-14	46.00%
GAWL01031818	Q5GIS3.1	gbb_pinfu ame: full=guanine nucleotide-binding protein subunit beta short=pfgbeta1 ame: full=g protein subunit beta-1	2638	1	6.10E-23	40.00%
GAWL01031982	Q5GIS3.1	gbb_pinfu ame: full=guanine nucleotide-binding protein subunit beta short=pfgbeta1 ame: full=g protein subunit	1831	1	6.80E-09	39.00%

		beta-1				
GAWL01034877	Q5GIS3.1	gbb_pinfu ame: full=guanine nucleotide-binding protein subunit beta short=pfgbeta1 ame: full=g protein subunit beta-1	1860	1	7.50E-17	42.00%
GAWL01034878	Q5GIS3.1	gbb_pinfu ame: full=guanine nucleotide-binding protein subunit beta short=pfgbeta1 ame: full=g protein subunit beta-1	1847	1	7.40E-17	42.00%
GAWL01040454	Q5GIS3.1	gbb_pinfu ame: full=guanine nucleotide-binding protein subunit beta short=pfgbeta1 ame: full=g protein subunit beta-1	1151	1	5.10E-17	43.00%
GAWL01040512	Q5GIS3.1	gbb_pinfu ame: full=guanine nucleotide-binding protein subunit beta short=pfgbeta1 ame: full=g protein subunit beta-1	1155	1	2.80E-11	37.00%
GAWL01040575	Q5GIS3.1	gbb_pinfu ame: full=guanine nucleotide-binding protein subunit beta short=pfgbeta1 ame: full=g protein subunit beta-1	1124	1	2.40E-12	39.00%
GAWL01040609	Q5GIS3.1	gbb_pinfu ame: full=guanine nucleotide-binding protein subunit beta short=pfgbeta1 ame: full=g protein subunit beta-1	1700	1	7.10E-22	43.00%
GAWL01043478	Q5GIS3.1	gbb_pinfu ame: full=guanine nucleotide-binding protein subunit beta short=pfgbeta1 ame: full=g protein subunit beta-1	375	1	9.20E-09	43.00%
GAWL01045568	Q5GIS3.1	gbb_pinfu ame: full=guanine nucleotide-binding protein subunit beta short=pfgbeta1 ame: full=g protein subunit beta-1	227	1	2.00E-09	45.00%
GAWL01002243	Q5GIS3.1	gbb_pinfu ame: full=guanine nucleotide-binding protein subunit beta short=pfgbeta1 ame: full=g protein subunit beta-1	1113	1	6.20E-26	44.00%
GAWL01002292	Q5GIS3.1	gbb_pinfu ame: full=guanine nucleotide-binding protein subunit beta short=pfgbeta1 ame: full=g protein subunit beta-1	963	1	3.50E-07	40.00%
GAWL01003348	Q5GIS3.1	gbb_pinfu ame: full=guanine nucleotide-binding protein subunit beta short=pfgbeta1 ame: full=g protein subunit beta-1	412	1	8.50E-10	44.00%
GAWL01003613	Q5GIS3.1	gbb_pinfu ame: full=guanine nucleotide-binding protein subunit beta short=pfgbeta1 ame: full=g protein subunit beta-1	314	1	4.00E-07	44.00%

GAWL01003614	Q5GIS3.1	gbb_pinfu ame: full=guanine nucleotide-binding protein subunit beta short=pfgbeta1 ame: full=g protein subunit beta-1	981	1	4.40E-18	44.00%
GAWL01003638	Q5GIS3.1	gbb_pinfu ame: full=guanine nucleotide-binding protein subunit beta short=pfgbeta1 ame: full=g protein subunit beta-1	945	1	1.20E-14	41.00%
GAWL01022590	P86785.1	giga2_cragi ame: full=gigasin-2 flags: precursor	2745	1	2.30E-16	42.00%
GAWL01043997	P86789.1	giga6_cragi ame: full=gigasin-6 flags: precursor	226	1	8.50E-16	62.00%
GAWL01045653	P86789.1	giga6_cragi ame: full=gigasin-6 flags: precursor	256	1	7.40E-08	55.00%
GAWL01032793	BAG50305.1	hypothetical protein	1694	1	2.70E-07	64.00%
GAWL01032794	BAG50305.1	hypothetical protein	1563	1	2.40E-07	64.00%
GAWL01023321	ADD16957.1	incilarin a	384	2	2.60E-08	43.00%
GAWL01023322	ADD16957.1	incilarin a	542	7	3.40E-17	43.43%
GAWL01009822	BAA19861.1	incilarin a	788	1	5.20E-08	43.00%
GAWL01010316	BAA19861.1	incilarin a	214	2	3.10E-07	47.50%
GAWL01013965	BAA19861.1	incilarin a	691	7	1.50E-17	44.29%
GAWL01015116	BAA19861.1	incilarin a	251	1	2.40E-07	50.00%
GAWL01019362	BAA19861.1	incilarin a	605	1	4.00E-08	44.00%
GAWL01020137	BAA19861.1	incilarin a	881	1	2.60E-07	39.00%
GAWL01021400	BAA19861.1	incilarin a	1054	1	9.20E-09	47.00%
GAWL01000570	BAA19861.1	incilarin a	215	1	4.40E-07	57.00%
GAWL01022500	BAA19861.1	incilarin a	651	7	8.60E-15	43.57%
GAWL01022939	BAA19861.1	incilarin a	2077	1	4.80E-08	41.00%
GAWL01024660	BAA19861.1	incilarin a	205	1	1.60E-09	53.00%
GAWL01025751	BAA19861.1	incilarin a	550	7	8.00E-19	44.14%
GAWL01027130	BAA19861.1	incilarin a	567	3	1.10E-09	46.33%
GAWL01027488	BAA19861.1	incilarin a	719	1	2.00E-10	48.00%
GAWL01027597	BAA19861.1	incilarin a	850	6	7.10E-17	43.00%
GAWL01027598	BAA19861.1	incilarin a	856	5	4.00E-17	44.20%
GAWL01027599	BAA19861.1	incilarin a	865	6	7.00E-17	43.00%
GAWL01027600	BAA19861.1	incilarin a	850	4	1.40E-16	43.00%

GAWL01027601	BAA19861.1	incilarin a	865	4	1.60E-16	43.00%
GAWL01027602	BAA19861.1	incilarin a	856	5	8.50E-17	44.00%
GAWL01027603	BAA19861.1	incilarin a	841	5	7.00E-17	44.00%
GAWL01027604	BAA19861.1	incilarin a	841	5	3.80E-17	44.20%
GAWL01033359	BAA19861.1	incilarin a	2123	4	6.20E-11	41.50%
GAWL01033361	BAA19861.1	incilarin a	2762	4	1.10E-10	41.00%
GAWL01033393	BAA19861.1	incilarin a	222	1	5.50E-07	56.00%
GAWL01040977	BAA19861.1	incilarin a	426	2	4.50E-10	49.00%
GAWL01042437	BAA19861.1	incilarin a	412	1	8.50E-08	44.00%
GAWL01001600	BAA19861.1	incilarin a	531	1	1.70E-09	47.00%
GAWL01004462	BAA19861.1	incilarin a	452	7	1.60E-19	44.57%
GAWL01004789	BAA19861.1	incilarin a	500	1	2.70E-09	49.00%
GAWL01016809	BAK86420.1	incilarin a	1117	4	2.50E-21	47.25%
GAWL01017803	BAK86420.1	incilarin a	2181	3	7.10E-25	44.67%
GAWL01009362	BAA19863.1	incilarin c	553	5	1.30E-08	47.20%
GAWL01022247	BAA19863.1	incilarin c	697	6	3.30E-19	44.33%
GAWL01022248	BAA19863.1	incilarin c	668	6	3.10E-19	44.83%
GAWL01024694	BAA19863.1	incilarin c	377	1	2.80E-07	42.00%
GAWL01025106	BAA19863.1	incilarin c	635	4	4.90E-12	40.75%
GAWL01025108	BAA19863.1	incilarin c	699	2	1.10E-10	53.00%
GAWL01003112	BAA19863.1	incilarin c	424	1	4.50E-08	50.00%
GAWL01005591	Q4KTY1.1	kpsh1_pinfu ame: full=serine threonine-protein kinase h1 homolog	1286	2	5.90E-43	52.00%
GAWL01008524	Q4KTY1.1	kpsh1_pinfu ame: full=serine threonine-protein kinase h1 homolog	328	2	7.30E-24	56.00%
GAWL01011705	Q4KTY1.1	kpsh1_pinfu ame: full=serine threonine-protein kinase h1 homolog	2192	2	2.40E-33	50.00%
GAWL01011706	Q4KTY1.1	kpsh1_pinfu ame: full=serine threonine-protein kinase h1 homolog	2176	2	2.30E-33	50.00%
GAWL01012100	Q4KTY1.1	kpsh1_pinfu ame: full=serine threonine-protein kinase h1 homolog	309	2	7.10E-28	60.00%

GAWL01012976	Q4KTY1.1	kpsh1_pinfu ame: full=serine threonine-protein kinase h1 homolog	290	1	6.90E-07	65.00%
GAWL01012977	Q4KTY1.1	kpsh1_pinfu ame: full=serine threonine-protein kinase h1 homolog	1312	2	5.20E-27	56.50%
GAWL01013823	Q4KTY1.1	kpsh1_pinfu ame: full=serine threonine-protein kinase h1 homolog	1071	2	2.10E-10	45.50%
GAWL01015085	Q4KTY1.1	kpsh1_pinfu ame: full=serine threonine-protein kinase h1 homolog	946	2	1.00E-33	52.00%
GAWL01017946	Q4KTY1.1	kpsh1_pinfu ame: full=serine threonine-protein kinase h1 homolog	793	2	3.50E-28	47.00%
GAWL01018390	Q4KTY1.1	kpsh1_pinfu ame: full=serine threonine-protein kinase h1 homolog	2337	2	8.20E-22	48.00%
GAWL01019103	Q4KTY1.1	kpsh1_pinfu ame: full=serine threonine-protein kinase h1 homolog	1434	2	4.50E-23	40.00%
GAWL01019277	Q4KTY1.1	kpsh1_pinfu ame: full=serine threonine-protein kinase h1 homolog	1811	2	6.60E-20	41.50%
GAWL01019446	Q4KTY1.1	kpsh1_pinfu ame: full=serine threonine-protein kinase h1 homolog	2890	2	1.50E-15	43.50%
GAWL01019593	Q4KTY1.1	kpsh1_pinfu ame: full=serine threonine-protein kinase h1 homolog	1114	3	2.00E-13	47.00%
GAWL01024755	Q4KTY1.1	kpsh1_pinfu ame: full=serine threonine-protein kinase h1 homolog	3215	2	1.60E-16	49.50%
GAWL01024893	Q4KTY1.1	kpsh1_pinfu ame: full=serine threonine-protein kinase h1 homolog	1469	2	2.90E-19	41.00%
GAWL01025488	Q4KTY1.1	kpsh1_pinfu ame: full=serine threonine-protein kinase h1 homolog	1618	2	8.70E-21	43.50%
GAWL01025489	Q4KTY1.1	kpsh1_pinfu ame: full=serine threonine-protein kinase h1 homolog	1306	2	4.50E-19	43.50%
GAWL01025490	Q4KTY1.1	kpsh1_pinfu ame: full=serine threonine-protein kinase h1 homolog	1602	2	8.80E-21	42.00%
GAWL01025491	Q4KTY1.1	kpsh1_pinfu ame: full=serine threonine-protein kinase h1 homolog	1322	2	6.70E-19	43.50%
GAWL01025493	Q4KTY1.1	kpsh1_pinfu ame: full=serine threonine-protein kinase h1 homolog	1293	2	1.40E-18	44.00%
GAWL01025495	Q4KTY1.1	kpsh1_pinfu ame: full=serine threonine-protein kinase h1 homolog	1277	2	9.00E-19	44.00%
GAWL01026117	Q4KTY1.1	kpsh1_pinfu ame: full=serine threonine-protein kinase h1 homolog	2891	2	2.40E-66	58.50%

GAWL01026772	Q4KTY1.1	kpsh1_pinfu ame: full=serine threonine-protein kinase h1 homolog	1496	2	7.40E-22	44.00%
GAWL01026773	Q4KTY1.1	kpsh1_pinfu ame: full=serine threonine-protein kinase h1 homolog	1360	2	5.50E-22	44.00%
GAWL01026774	Q4KTY1.1	kpsh1_pinfu ame: full=serine threonine-protein kinase h1 homolog	1514	2	7.60E-22	44.00%
GAWL01026775	Q4KTY1.1	kpsh1_pinfu ame: full=serine threonine-protein kinase h1 homolog	1342	2	5.30E-22	44.00%
GAWL01026909	Q4KTY1.1	kpsh1_pinfu ame: full=serine threonine-protein kinase h1 homolog	1532	2	1.30E-20	42.00%
GAWL01028721	Q4KTY1.1	kpsh1_pinfu ame: full=serine threonine-protein kinase h1 homolog	2709	3	6.90E-42	47.00%
GAWL01028743	Q4KTY1.1	kpsh1_pinfu ame: full=serine threonine-protein kinase h1 homolog	2708	2	1.10E-33	50.00%
GAWL01029378	Q4KTY1.1	kpsh1_pinfu ame: full=serine threonine-protein kinase h1 homolog	1220	2	1.10E-21	43.00%
GAWL01032063	Q4KTY1.1	kpsh1_pinfu ame: full=serine threonine-protein kinase h1 homolog	1418	2	3.40E-21	44.00%
GAWL01036701	Q4KTY1.1	kpsh1_pinfu ame: full=serine threonine-protein kinase h1 homolog	2106	1	2.00E-10	45.00%
GAWL01036743	Q4KTY1.1	kpsh1_pinfu ame: full=serine threonine-protein kinase h1 homolog	2083	2	6.80E-69	55.00%
GAWL01038312	Q4KTY1.1	kpsh1_pinfu ame: full=serine threonine-protein kinase h1 homolog	3048	2	4.60E-17	43.50%
GAWL01038313	Q4KTY1.1	kpsh1_pinfu ame: full=serine threonine-protein kinase h1 homolog	2809	2	4.10E-17	43.50%
GAWL01038314	Q4KTY1.1	kpsh1_pinfu ame: full=serine threonine-protein kinase h1 homolog	1375	2	1.40E-15	43.50%
GAWL01038315	Q4KTY1.1	kpsh1_pinfu ame: full=serine threonine-protein kinase h1 homolog	2850	2	4.20E-17	43.50%
GAWL01038316	Q4KTY1.1	kpsh1_pinfu ame: full=serine threonine-protein kinase h1 homolog	3082	2	4.70E-17	43.50%
GAWL01038302	Q4KTY1.1	kpsh1_pinfu ame: full=serine threonine-protein kinase h1 homolog	2816	2	4.20E-17	43.50%
GAWL01038305	Q4KTY1.1	kpsh1_pinfu ame: full=serine threonine-protein kinase h1 homolog	1368	2	1.40E-15	43.50%
GAWL01038306	Q4KTY1.1	kpsh1_pinfu ame: full=serine threonine-protein kinase h1 homolog	1607	2	1.90E-15	43.50%

GAWL01038307	Q4KTY1.1	kpsh1_pinfu ame: full=serine threonine-protein kinase h1 homolog	2843	2	4.20E-17	43.50%
GAWL01040641	Q4KTY1.1	kpsh1_pinfu ame: full=serine threonine-protein kinase h1 homolog	1185	3	2.70E-16	43.33%
GAWL01014846	BAB03232.1	lectin	281	1	1.10E-07	45.00%
GAWL01026700	BAB03232.1	lectin	1066	1	2.10E-10	40.00%
GAWL01026702	BAB03232.1	lectin	930	1	2.30E-10	40.00%
GAWL01032172	BAB03232.1	lectin	855	1	7.40E-07	37.00%
GAWL01038774	BAB03232.1	lectin	419	1	2.40E-07	38.00%
GAWL01005365	AAZ76256.1	mantle gene 2	3103	1	6.10E-30	56.00%
GAWL01024519	AAZ76256.1	mantle gene 2	2012	1	1.30E-43	60.00%
GAWL01024528	AAZ76256.1	mantle gene 2	1917	1	8.30E-44	60.00%
GAWL01024520	AAZ76256.1	mantle gene 2	1969	1	9.50E-44	60.00%
GAWL01024521	AAZ76256.1	mantle gene 2	2025	1	1.40E-43	60.00%
GAWL01024523	AAZ76256.1	mantle gene 2	1930	1	8.50E-44	60.00%
GAWL01024524	AAZ76256.1	mantle gene 2	1973	1	1.20E-43	60.00%
GAWL01024526	AAZ76256.1	mantle gene 2	1986	1	1.20E-43	60.00%
GAWL01024527	AAZ76256.1	mantle gene 2	1956	1	9.20E-44	60.00%
GAWL01024644	AAZ76256.1	mantle gene 2	1413	1	2.10E-30	57.00%
GAWL01000721	AAZ76256.1	mantle gene 2	842	1	1.70E-33	53.00%
GAWL01013527	AAZ76258.1	mantle gene 4	296	2	6.10E-10	50.50%
GAWL01016048	AAZ76258.1	mantle gene 4	447	1	1.70E-11	52.00%
GAWL01016885	AAZ76258.1	mantle gene 4	398	1	2.90E-08	42.00%
GAWL01018299	AAZ76258.1	mantle gene 4	591	1	6.10E-13	46.00%
GAWL01019616	AAZ76258.1	mantle gene 4	663	2	4.90E-12	48.50%
GAWL01019617	AAZ76258.1	mantle gene 4	766	2	5.50E-11	48.00%
GAWL01020124	AAZ76258.1	mantle gene 4	753	2	1.80E-08	47.00%
GAWL01020878	AAZ76258.1	mantle gene 4	682	2	6.80E-10	45.00%
GAWL01020879	AAZ76258.1	mantle gene 4	682	2	5.60E-09	47.00%
GAWL01020880	AAZ76258.1	mantle gene 4	692	2	1.60E-08	45.00%

GAWL01023259	AAZ76258.1	mantle gene 4	726	2	2.00E-09	43.00%
GAWL01024194	AAZ76258.1	mantle gene 4	1428	1	1.20E-12	50.00%
GAWL01024195	AAZ76258.1	mantle gene 4	904	1	4.20E-13	50.00%
GAWL01024196	AAZ76258.1	mantle gene 4	863	1	3.60E-13	50.00%
GAWL01025730	AAZ76258.1	mantle gene 4	1128	2	2.20E-11	47.50%
GAWL01025704	AAZ76258.1	mantle gene 4	666	3	1.00E-09	53.67%
GAWL01025735	AAZ76258.1	mantle gene 4	802	3	1.80E-11	51.67%
GAWL01025705	AAZ76258.1	mantle gene 4	896	3	2.40E-11	51.67%
GAWL01025706	AAZ76258.1	mantle gene 4	1140	2	2.30E-11	47.50%
GAWL01029052	AAZ76258.1	mantle gene 4	554	2	5.30E-15	53.00%
GAWL01029053	AAZ76258.1	mantle gene 4	690	2	6.60E-15	53.00%
GAWL01029201	AAZ76258.1	mantle gene 4	870	1	3.30E-10	44.00%
GAWL01038311	AAZ76258.1	mantle gene 4	675	2	4.20E-15	47.00%
GAWL01038303	AAZ76258.1	mantle gene 4	1021	2	1.10E-15	51.00%
GAWL01043139	AAZ76258.1	mantle gene 4	320	1	4.30E-11	48.00%
GAWL01045393	AAZ76258.1	mantle gene 4	225	1	9.40E-07	54.00%
GAWL01000774	AAZ76258.1	mantle gene 4	573	2	1.30E-12	48.50%
GAWL01001165	AAZ76258.1	mantle gene 4	621	2	2.10E-13	47.50%
GAWL01002324	AAZ76258.1	mantle gene 4	639	2	5.30E-14	50.00%
GAWL01004039	AAZ76258.1	mantle gene 4	577	2	3.90E-13	46.50%
GAWL01018251	AAZ22321.1	mantle protein 12	938	1	2.70E-07	61.00%
GAWL01023722	AAZ22321.1	mantle protein 12	1292	1	7.40E-08	71.00%
GAWL01023723	AAZ22321.1	mantle protein 12	1306	1	7.50E-08	71.00%
GAWL01023724	AAZ22321.1	mantle protein 12	1179	1	6.50E-08	71.00%
GAWL01023725	AAZ22321.1	mantle protein 12	1144	1	6.30E-08	71.00%
GAWL01023728	AAZ22321.1	mantle protein 12	273	1	1.20E-07	56.00%
GAWL01026543	AAZ22321.1	mantle protein 12	689	1	3.30E-09	61.00%
GAWL01036679	AAZ22321.1	mantle protein 12	511	1	5.50E-08	52.00%
GAWL01036680	AAZ22321.1	mantle protein 12	551	1	6.90E-08	52.00%

GAWL01042619	AAZ22321.1	mantle protein 12	281	1	2.70E-07	55.00%
GAWL01019096	AAZ22318.1	mantle protein 9	616	1	7.50E-12	39.00%
GAWL01020454	AAZ22318.1	mantle protein 9	497	1	2.40E-09	43.00%
GAWL01020747	AAZ22318.1	mantle protein 9	612	1	8.20E-08	44.00%
GAWL01023863	AAZ22318.1	mantle protein 9	763	1	2.10E-09	43.00%
GAWL01010347	AAZ66779.2	neuronal calcium sensor-1	790	5	1.40E-32	52.40%
GAWL01020837	AAZ66779.2	neuronal calcium sensor-1	1118	5	1.20E-33	52.40%
GAWL01020838	AAZ66779.2	neuronal calcium sensor-1	960	5	5.80E-34	52.40%
GAWL01020839	AAZ66779.2	neuronal calcium sensor-1	1185	5	1.60E-39	52.60%
GAWL01022901	AAZ66779.2	neuronal calcium sensor-1	754	1	1.90E-26	51.00%
GAWL01025827	AAZ66779.2	neuronal calcium sensor-1	1576	2	2.90E-32	55.00%
GAWL01025828	AAZ66779.2	neuronal calcium sensor-1	1043	2	4.60E-23	56.00%
GAWL01027469	AAZ66779.2	neuronal calcium sensor-1	1069	4	9.40E-16	46.75%
GAWL01027470	AAZ66779.2	neuronal calcium sensor-1	1195	3	2.80E-22	49.33%
GAWL01027471	AAZ66779.2	neuronal calcium sensor-1	1207	1	5.60E-10	46.00%
GAWL01033972	AAZ66779.2	neuronal calcium sensor-1	961	3	1.90E-34	51.67%
GAWL01044474	AAZ66779.2	neuronal calcium sensor-1	290	1	3.80E-12	53.00%
GAWL01009425	ADD16957.1	perlucin	413	1	6.10E-08	43.00%
GAWL01019723	ADD16957.1	perlucin	873	1	2.80E-08	53.00%
GAWL01032648	ADD16957.1	perlucin	258	1	3.10E-08	50.00%
GAWL01037379	ADD16957.1	perlucin	277	1	5.10E-07	46.00%
GAWL01038894	ADD16957.1	perlucin	1664	1	8.70E-08	44.00%
GAWL01038903	ADD16957.1	perlucin	1641	1	1.00E-07	45.00%
GAWL01038886	ADD16957.1	perlucin	2213	1	9.90E-08	44.00%
GAWL01038909	ADD16957.1	perlucin	2190	1	1.30E-07	45.00%
GAWL01006699	ABO26596.1	perlucin 7	1135	6	8.80E-12	43.00%
GAWL01007441	ABO26596.1	perlucin 7	370	2	1.50E-08	45.00%
GAWL01007554	ABO26596.1	perlucin 7	494	1	6.50E-07	53.00%
GAWL01010244	ABO26596.1	perlucin 7	225	1	6.70E-07	50.00%

GAWL01012361	ABO26596.1	perlucin 7	820	1	3.20E-07	43.00%
GAWL01013456	ABO26596.1	perlucin 7	276	4	1.20E-12	51.50%
GAWL01016387	ABO26596.1	perlucin 7	796	6	3.60E-14	43.17%
GAWL01016388	ABO26596.1	perlucin 7	781	6	3.30E-14	43.17%
GAWL01017017	ABO26596.1	perlucin 7	649	7	6.60E-15	44.29%
GAWL01018152	ABO26596.1	perlucin 7	990	4	8.50E-13	41.50%
GAWL01022940	ABO26596.1	perlucin 7	1280	1	5.50E-07	44.00%
GAWL01023222	ABO26596.1	perlucin 7	1861	2	2.60E-07	42.50%
GAWL01023524	ABO26596.1	perlucin 7	1785	3	2.00E-14	45.00%
GAWL01023526	ABO26596.1	perlucin 7	1760	3	1.60E-14	45.00%
GAWL01023865	ABO26596.1	perlucin 7	613	3	1.80E-09	44.33%
GAWL01024432	ABO26596.1	perlucin 7	1014	2	2.70E-13	46.50%
GAWL01024434	ABO26596.1	perlucin 7	1147	2	3.30E-13	46.50%
GAWL01026679	ABO26596.1	perlucin 7	1058	1	7.10E-11	41.00%
GAWL01026680	ABO26596.1	perlucin 7	1018	1	1.40E-12	41.00%
GAWL01027728	ABO26596.1	perlucin 7	1780	3	1.50E-08	41.67%
GAWL01027729	ABO26596.1	perlucin 7	1149	3	9.10E-09	41.67%
GAWL01029301	ABO26596.1	perlucin 7	1092	5	1.80E-11	39.00%
GAWL01032250	ABO26596.1	perlucin 7	1267	4	6.10E-10	42.50%
GAWL01033150	ABO26596.1	perlucin 7	1733	1	1.90E-10	46.00%
GAWL01033151	ABO26596.1	perlucin 7	1701	1	1.80E-10	44.00%
GAWL01033154	ABO26596.1	perlucin 7	824	2	1.20E-11	42.00%
GAWL01033494	ABO26596.1	perlucin 7	2261	6	1.40E-12	43.00%
GAWL01033495	ABO26596.1	perlucin 7	2272	6	1.40E-12	43.00%
GAWL01034205	ABO26596.1	perlucin 7	803	5	9.20E-17	46.00%
GAWL01034206	ABO26596.1	perlucin 7	598	6	2.50E-15	44.00%
GAWL01034407	ABO26596.1	perlucin 7	350	2	5.30E-11	44.50%
GAWL01034782	ABO26596.1	perlucin 7	1861	5	6.10E-13	45.00%
GAWL01034785	ABO26596.1	perlucin 7	1817	5	5.90E-13	45.00%

GAWL01036328	ABO26596.1	perlucin 7	3004	4	1.30E-10	46.00%
GAWL01036329	ABO26596.1	perlucin 7	2977	4	1.10E-10	46.00%
GAWL01036330	ABO26596.1	perlucin 7	2602	4	1.50E-10	46.00%
GAWL01036332	ABO26596.1	perlucin 7	1845	5	1.60E-12	45.40%
GAWL01036335	ABO26596.1	perlucin 7	2614	4	1.20E-10	46.00%
GAWL01036336	ABO26596.1	perlucin 7	2641	4	1.20E-10	46.00%
GAWL01038777	ABO26596.1	perlucin 7	413	2	3.40E-10	51.50%
GAWL01038778	ABO26596.1	perlucin 7	585	2	1.00E-09	51.50%
GAWL01041002	ABO26596.1	perlucin 7	796	5	2.80E-20	47.00%
GAWL01041183	ABO26596.1	perlucin 7	468	5	7.30E-15	41.60%
GAWL01005093	ABO26596.1	perlucin 7	303	3	2.60E-11	52.33%
GAWL01011701	ADD16957.1	perlucin 7	515	7	1.70E-21	46.29%
GAWL01017902	ADD16957.1	perlucin 7	605	2	9.90E-12	45.00%
GAWL01001834	ADD16957.1	perlucin 7	545	2	1.30E-08	41.50%
GAWL01033432	ABL63470.1	plasma membrane calcium atpase	3939	3	0.00E+00	57.00%
GAWL01033433	ABL63470.1	plasma membrane calcium atpase	3972	3	0.00E+00	57.33%
GAWL01033434	ABL63470.1	plasma membrane calcium atpase	2817	3	0.00E+00	56.33%
GAWL01033435	ABL63470.1	plasma membrane calcium atpase	2850	3	0.00E+00	56.33%
GAWL01015434	ADD16957.1	plc_halla ame: full=perlucin	788	4	9.70E-12	40.75%
GAWL01015435	ADD16957.1	plc_halla ame: full=perlucin	813	4	1.10E-11	40.75%
GAWL01023326	ADD16957.1	plc_halla ame: full=perlucin	850	5	1.70E-15	42.80%
GAWL01027506	ADD16957.1	plc_halla ame: full=perlucin	1044	7	6.90E-17	45.57%
GAWL01029186	ADD16957.1	plc_halla ame: full=perlucin	1774	2	8.30E-09	44.00%
GAWL01032658	ADD16957.1	plc_halla ame: full=perlucin	709	2	1.30E-11	47.00%
GAWL01032669	ADD16957.1	plc_halla ame: full=perlucin	551	7	2.30E-22	47.43%
GAWL01035992	ADD16957.1	plc_halla ame: full=perlucin	1579	2	1.20E-10	39.50%
GAWL01035982	ADD16957.1	plc_halla ame: full=perlucin	1534	2	1.20E-10	39.50%
GAWL01040736	ADD16957.1	plc_halla ame: full=perlucin	476	5	6.90E-16	45.80%
GAWL01005275	ADD16957.1	plc_halla ame: full=perlucin	630	6	2.80E-14	43.00%

GAWL01005347	P82596.3	plc_halla ame: full=perlucin	580	3	2.70E-10	42.00%
GAWL01005480	P82596.3	plc_halla ame: full=perlucin	690	6	7.40E-20	44.17%
GAWL01005810	P82596.3	plc_halla ame: full=perlucin	589	7	1.30E-21	46.86%
GAWL01005831	P82596.3	plc_halla ame: full=perlucin	499	7	2.00E-18	44.57%
GAWL01006141	P82596.3	plc_halla ame: full=perlucin	450	6	9.70E-19	43.17%
GAWL01006160	P82596.3	plc_halla ame: full=perlucin	537	5	2.20E-18	44.00%
GAWL01006190	P82596.3	plc_halla ame: full=perlucin	739	7	3.00E-18	44.43%
GAWL01006557	P82596.3	plc_halla ame: full=perlucin	1353	7	4.10E-13	43.71%
GAWL01006612	P82596.3	plc_halla ame: full=perlucin	566	3	2.00E-11	42.67%
GAWL01006836	P82596.3	plc_halla ame: full=perlucin	537	4	5.20E-13	46.00%
GAWL01007010	P82596.3	plc_halla ame: full=perlucin	1043	6	1.50E-15	45.17%
GAWL01007457	P82596.3	plc_halla ame: full=perlucin	442	5	1.10E-13	41.80%
GAWL01007748	P82596.3	plc_halla ame: full=perlucin	349	2	4.20E-11	47.00%
GAWL01008118	P82596.3	plc_halla ame: full=perlucin	514	6	5.60E-17	44.33%
GAWL01008327	P82596.3	plc_halla ame: full=perlucin	330	5	1.40E-14	51.40%
GAWL01008500	P82596.3	plc_halla ame: full=perlucin	518	4	8.20E-13	41.00%
GAWL01008862	P82596.3	plc_halla ame: full=perlucin	584	7	8.20E-24	45.57%
GAWL01009030	P82596.3	plc_halla ame: full=perlucin	208	1	5.80E-07	48.00%
GAWL01009239	P82596.3	plc_halla ame: full=perlucin	394	5	1.10E-13	47.60%
GAWL01009321	P82596.3	plc_halla ame: full=perlucin	628	1	1.50E-07	47.00%
GAWL01009948	P82596.3	plc_halla ame: full=perlucin	645	1	2.80E-09	45.00%
GAWL01010243	P82596.3	plc_halla ame: full=perlucin	422	1	2.40E-10	55.00%
GAWL01010364	P82596.3	plc_halla ame: full=perlucin	301	4	8.60E-10	46.50%
GAWL01011095	P82596.3	plc_halla ame: full=perlucin	563	7	6.50E-17	41.57%
GAWL01011139	P82596.3	plc_halla ame: full=perlucin	402	7	1.00E-16	44.71%
GAWL01011399	P82596.3	plc_halla ame: full=perlucin	375	1	4.90E-09	53.00%
GAWL01011400	P82596.3	plc_halla ame: full=perlucin	531	1	3.40E-07	48.00%
GAWL01011500	P82596.3	plc_halla ame: full=perlucin	552	2	2.90E-10	40.50%
GAWL01012148	P82596.3	plc_halla ame: full=perlucin	349	6	5.40E-16	46.00%

GAWL01012183	P82596.3	plc_halla ame: full=perlucin	381	2	3.50E-09	46.00%
GAWL01012184	P82596.3	plc_halla ame: full=perlucin	367	3	1.20E-09	45.33%
GAWL01013378	P82596.3	plc_halla ame: full=perlucin	635	7	6.60E-22	47.00%
GAWL01013984	P82596.3	plc_halla ame: full=perlucin	497	1	1.00E-11	51.00%
GAWL01014157	P82596.3	plc_halla ame: full=perlucin	255	2	7.90E-08	53.00%
GAWL01014787	P82596.3	plc_halla ame: full=perlucin	219	3	2.80E-10	53.33%
GAWL01015346	P82596.3	plc_halla ame: full=perlucin	335	1	3.50E-08	51.00%
GAWL01015444	P82596.3	plc_halla ame: full=perlucin	619	7	4.40E-18	44.29%
GAWL01015909	P82596.3	plc_halla ame: full=perlucin	665	3	3.00E-12	43.67%
GAWL01015910	P82596.3	plc_halla ame: full=perlucin	629	4	1.40E-14	43.25%
GAWL01016464	P82596.3	plc_halla ame: full=perlucin	754	2	5.00E-13	42.50%
GAWL01016832	P82596.3	plc_halla ame: full=perlucin	558	7	4.10E-24	45.29%
GAWL01016889	P82596.3	plc_halla ame: full=perlucin	528	7	1.60E-23	45.00%
GAWL01017308	P82596.3	plc_halla ame: full=perlucin	888	1	9.60E-12	42.00%
GAWL01017309	P82596.3	plc_halla ame: full=perlucin	867	2	6.60E-12	41.00%
GAWL01017761	P82596.3	plc_halla ame: full=perlucin	432	3	2.90E-09	45.00%
GAWL01018151	P82596.3	plc_halla ame: full=perlucin	1107	5	1.00E-11	42.60%
GAWL01018326	P82596.3	plc_halla ame: full=perlucin	624	7	7.60E-21	46.00%
GAWL01018595	P82596.3	plc_halla ame: full=perlucin	291	1	4.00E-07	45.00%
GAWL01018983	P82596.3	plc_halla ame: full=perlucin	2211	7	4.10E-15	45.00%
GAWL01019170	P82596.3	plc_halla ame: full=perlucin	538	6	8.90E-17	47.17%
GAWL01019822	P82596.3	plc_halla ame: full=perlucin	630	6	2.60E-15	41.83%
GAWL01019823	P82596.3	plc_halla ame: full=perlucin	533	7	1.10E-19	44.00%
GAWL01020037	P82596.3	plc_halla ame: full=perlucin	872	1	7.10E-07	53.00%
GAWL01020100	P82596.3	plc_halla ame: full=perlucin	538	7	1.30E-18	44.57%
GAWL01020495	P82596.3	plc_halla ame: full=perlucin	567	7	4.20E-16	43.14%
GAWL01020728	P82596.3	plc_halla ame: full=perlucin	683	3	1.90E-10	47.67%
GAWL01020729	P82596.3	plc_halla ame: full=perlucin	704	3	2.50E-10	47.67%
GAWL01022592	P82596.3	plc_halla ame: full=perlucin	255	1	7.50E-10	47.00%

GAWL01022681	P82596.3	plc_halla ame: full=perlucin	431	4	1.10E-18	46.25%
GAWL01022682	P82596.3	plc_halla ame: full=perlucin	562	4	2.40E-18	46.25%
GAWL01023311	P82596.3	plc_halla ame: full=perlucin	879	3	9.60E-11	41.33%
GAWL01023325	P82596.3	plc_halla ame: full=perlucin	852	6	8.40E-12	41.83%
GAWL01023395	P82596.3	plc_halla ame: full=perlucin	672	6	5.40E-22	46.67%
GAWL01023523	P82596.3	plc_halla ame: full=perlucin	1785	3	1.60E-12	44.00%
GAWL01023525	P82596.3	plc_halla ame: full=perlucin	1760	3	4.40E-13	43.67%
GAWL01024350	P82596.3	plc_halla ame: full=perlucin	492	1	1.80E-07	55.00%
GAWL01024548	P82596.3	plc_halla ame: full=perlucin	3672	2	2.50E-10	46.50%
GAWL01024603	P82596.3	plc_halla ame: full=perlucin	893	2	1.40E-10	43.00%
GAWL01024659	P82596.3	plc_halla ame: full=perlucin	213	4	6.00E-11	48.75%
GAWL01024661	P82596.3	plc_halla ame: full=perlucin	274	1	1.20E-07	63.00%
GAWL01024758	P82596.3	plc_halla ame: full=perlucin	549	7	7.80E-25	47.14%
GAWL01024759	P82596.3	plc_halla ame: full=perlucin	733	7	4.60E-17	47.43%
GAWL01025067	P82596.3	plc_halla ame: full=perlucin	1125	7	3.40E-18	45.57%
GAWL01025068	P82596.3	plc_halla ame: full=perlucin	927	7	2.10E-18	45.43%
GAWL01025071	P82596.3	plc_halla ame: full=perlucin	1112	7	3.20E-18	45.57%
GAWL01025072	P82596.3	plc_halla ame: full=perlucin	1558	8	2.40E-16	44.25%
GAWL01025140	P82596.3	plc_halla ame: full=perlucin	1026	6	1.60E-12	42.33%
GAWL01025145	P82596.3	plc_halla ame: full=perlucin	1006	6	5.20E-19	46.00%
GAWL01025147	P82596.3	plc_halla ame: full=perlucin	979	6	2.70E-19	46.17%
GAWL01025412	P82596.3	plc_halla ame: full=perlucin	640	2	2.30E-11	44.50%
GAWL01025441	P82596.3	plc_halla ame: full=perlucin	927	3	2.20E-09	45.67%
GAWL01025702	P82596.3	plc_halla ame: full=perlucin	838	6	1.90E-17	46.00%
GAWL01025712	P82596.3	plc_halla ame: full=perlucin	742	6	1.70E-18	46.00%
GAWL01025720	P82596.3	plc_halla ame: full=perlucin	389	3	7.70E-15	49.33%
GAWL01025722	P82596.3	plc_halla ame: full=perlucin	881	6	2.10E-15	46.50%
GAWL01025724	P82596.3	plc_halla ame: full=perlucin	803	4	5.20E-16	50.50%
GAWL01025726	P82596.3	plc_halla ame: full=perlucin	826	6	2.20E-17	46.00%

GAWL01025732	P82596.3	plc_halla ame: full=perlucin	754	6	1.30E-18	46.17%
GAWL01025707	P82596.3	plc_halla ame: full=perlucin	797	6	1.30E-16	46.17%
GAWL01027188	P82596.3	plc_halla ame: full=perlucin	1026	4	2.40E-11	46.75%
GAWL01027189	P82596.3	plc_halla ame: full=perlucin	1571	4	1.10E-11	46.75%
GAWL01028246	P82596.3	plc_halla ame: full=perlucin	1135	1	8.40E-09	45.00%
GAWL01029026	P82596.3	plc_halla ame: full=perlucin	448	1	9.00E-08	52.00%
GAWL01029029	P82596.3	plc_halla ame: full=perlucin	307	2	7.60E-12	48.00%
GAWL01029153	P82596.3	plc_halla ame: full=perlucin	627	1	1.20E-08	44.00%
GAWL01029161	P82596.3	plc_halla ame: full=perlucin	896	5	2.90E-15	43.00%
GAWL01029162	P82596.3	plc_halla ame: full=perlucin	795	3	9.20E-13	43.33%
GAWL01029184	P82596.3	plc_halla ame: full=perlucin	2438	2	9.40E-11	46.50%
GAWL01029261	P82596.3	plc_halla ame: full=perlucin	834	4	7.20E-12	42.75%
GAWL01029262	P82596.3	plc_halla ame: full=perlucin	1680	4	4.60E-11	42.75%
GAWL01029263	P82596.3	plc_halla ame: full=perlucin	1662	4	1.20E-12	44.00%
GAWL01029494	P82596.3	plc_halla ame: full=perlucin	629	7	5.00E-13	43.57%
GAWL01029499	P82596.3	plc_halla ame: full=perlucin	770	7	1.30E-12	44.00%
GAWL01029778	P82596.3	plc_halla ame: full=perlucin	264	1	1.10E-07	45.00%
GAWL01029789	P82596.3	plc_halla ame: full=perlucin	206	1	2.60E-07	49.00%
GAWL01030073	P82596.3	plc_halla ame: full=perlucin	416	2	4.60E-09	50.00%
GAWL01030074	P82596.3	plc_halla ame: full=perlucin	442	2	7.30E-09	48.50%
GAWL01030079	P82596.3	plc_halla ame: full=perlucin	310	2	5.40E-13	49.50%
GAWL01030080	P82596.3	plc_halla ame: full=perlucin	446	5	2.00E-09	44.20%
GAWL01030167	P82596.3	plc_halla ame: full=perlucin	674	6	3.10E-19	43.17%
GAWL01030229	P82596.3	plc_halla ame: full=perlucin	1773	5	4.40E-16	45.20%
GAWL01030231	P82596.3	plc_halla ame: full=perlucin	1530	5	3.20E-16	45.20%
GAWL01030223	P82596.3	plc_halla ame: full=perlucin	1019	5	7.20E-17	45.20%
GAWL01030226	P82596.3	plc_halla ame: full=perlucin	1262	5	1.50E-16	45.20%
GAWL01031304	P82596.3	plc_halla ame: full=perlucin	1041	1	5.30E-07	43.00%
GAWL01032646	P82596.3	plc_halla ame: full=perlucin	596	5	1.80E-12	44.40%

GAWL01032656	P82596.3	plc_halla ame: full=perlucin	376	4	1.90E-12	50.50%
GAWL01032657	P82596.3	plc_halla ame: full=perlucin	274	3	1.00E-09	53.00%
GAWL01032659	P82596.3	plc_halla ame: full=perlucin	226	1	1.80E-07	55.00%
GAWL01032660	P82596.3	plc_halla ame: full=perlucin	562	7	5.80E-20	46.86%
GAWL01032661	P82596.3	plc_halla ame: full=perlucin	564	5	3.10E-12	44.60%
GAWL01032662	P82596.3	plc_halla ame: full=perlucin	552	5	7.20E-12	43.60%
GAWL01032664	P82596.3	plc_halla ame: full=perlucin	572	5	1.70E-12	44.40%
GAWL01032647	P82596.3	plc_halla ame: full=perlucin	512	1	6.20E-07	53.00%
GAWL01032667	P82596.3	plc_halla ame: full=perlucin	281	6	3.70E-15	48.83%
GAWL01032668	P82596.3	plc_halla ame: full=perlucin	620	7	9.10E-22	48.00%
GAWL01032649	P82596.3	plc_halla ame: full=perlucin	314	6	3.90E-11	53.67%
GAWL01032651	P82596.3	plc_halla ame: full=perlucin	560	4	3.90E-12	44.75%
GAWL01032654	P82596.3	plc_halla ame: full=perlucin	584	4	4.00E-12	44.75%
GAWL01032716	P82596.3	plc_halla ame: full=perlucin	944	1	6.30E-07	44.00%
GAWL01032872	P82596.3	plc_halla ame: full=perlucin	294	3	1.40E-12	54.67%
GAWL01033357	P82596.3	plc_halla ame: full=perlucin	969	3	5.80E-12	42.67%
GAWL01033360	P82596.3	plc_halla ame: full=perlucin	1384	2	3.40E-12	44.00%
GAWL01033362	P82596.3	plc_halla ame: full=perlucin	745	2	6.50E-13	45.00%
GAWL01033363	P82596.3	plc_halla ame: full=perlucin	1436	3	1.40E-09	42.00%
GAWL01033392	P82596.3	plc_halla ame: full=perlucin	352	1	2.40E-11	48.00%
GAWL01033403	P82596.3	plc_halla ame: full=perlucin	560	5	6.20E-11	47.40%
GAWL01033406	P82596.3	plc_halla ame: full=perlucin	595	4	7.50E-11	47.75%
GAWL01033408	P82596.3	plc_halla ame: full=perlucin	702	3	2.50E-10	47.33%
GAWL01033394	P82596.3	plc_halla ame: full=perlucin	702	3	2.60E-10	47.33%
GAWL01033398	P82596.3	plc_halla ame: full=perlucin	894	3	5.30E-10	47.33%
GAWL01034413	P82596.3	plc_halla ame: full=perlucin	445	1	2.30E-07	41.00%
GAWL01034414	P82596.3	plc_halla ame: full=perlucin	632	6	3.50E-15	41.33%
GAWL01034617	P82596.3	plc_halla ame: full=perlucin	733	2	4.10E-09	45.00%
GAWL01035031	P82596.3	plc_halla ame: full=perlucin	688	4	1.00E-13	44.75%

GAWL01035200	P82596.3	plc_halla ame: full=perlucin	368	3	5.40E-11	49.67%
GAWL01035665	P82596.3	plc_halla ame: full=perlucin	469	1	8.40E-07	49.00%
GAWL01036337	P82596.3	plc_halla ame: full=perlucin	2587	1	3.40E-07	48.00%
GAWL01036333	P82596.3	plc_halla ame: full=perlucin	2224	1	4.40E-07	45.00%
GAWL01036334	P82596.3	plc_halla ame: full=perlucin	2212	1	6.90E-09	48.00%
GAWL01036730	P82596.3	plc_halla ame: full=perlucin	1922	5	1.10E-11	42.80%
GAWL01036731	P82596.3	plc_halla ame: full=perlucin	1796	5	9.90E-12	42.80%
GAWL01036732	P82596.3	plc_halla ame: full=perlucin	1924	5	1.00E-11	42.80%
GAWL01036734	P82596.3	plc_halla ame: full=perlucin	1824	5	1.00E-11	42.80%
GAWL01036735	P82596.3	plc_halla ame: full=perlucin	1809	5	1.00E-11	42.80%
GAWL01036736	P82596.3	plc_halla ame: full=perlucin	2064	4	1.90E-11	43.50%
GAWL01036737	P82596.3	plc_halla ame: full=perlucin	1811	5	1.00E-11	42.80%
GAWL01036726	P82596.3	plc_halla ame: full=perlucin	1951	4	1.90E-11	43.50%
GAWL01036728	P82596.3	plc_halla ame: full=perlucin	1937	5	1.00E-11	42.80%
GAWL01036729	P82596.3	plc_halla ame: full=perlucin	1909	5	1.10E-11	42.80%
GAWL01037310	P82596.3	plc_halla ame: full=perlucin	889	3	2.70E-11	43.67%
GAWL01037311	P82596.3	plc_halla ame: full=perlucin	727	3	1.50E-11	43.67%
GAWL01037313	P82596.3	plc_halla ame: full=perlucin	489	3	1.70E-12	44.33%
GAWL01037303	P82596.3	plc_halla ame: full=perlucin	1081	3	4.00E-11	43.67%
GAWL01037309	P82596.3	plc_halla ame: full=perlucin	1295	3	5.50E-11	43.67%
GAWL01037387	P82596.3	plc_halla ame: full=perlucin	329	2	2.00E-09	46.50%
GAWL01037390	P82596.3	plc_halla ame: full=perlucin	246	2	1.10E-10	47.00%
GAWL01037394	P82596.3	plc_halla ame: full=perlucin	383	3	4.60E-11	45.00%
GAWL01037399	P82596.3	plc_halla ame: full=perlucin	582	1	3.20E-11	53.00%
GAWL01037401	P82596.3	plc_halla ame: full=perlucin	258	2	1.70E-10	46.50%
GAWL01037462	P82596.3	plc_halla ame: full=perlucin	2819	5	1.50E-15	45.60%
GAWL01039232	P82596.3	plc_halla ame: full=perlucin	2078	1	8.20E-10	46.00%
GAWL01039223	P82596.3	plc_halla ame: full=perlucin	2417	3	2.20E-14	41.67%
GAWL01039228	P82596.3	plc_halla ame: full=perlucin	1285	6	1.60E-14	42.83%

GAWL01039230	P82596.3	plc_halla ame: full=perlucin	3640	1	6.30E-08	43.00%
GAWL01039567	P82596.3	plc_halla ame: full=perlucin	1800	5	4.20E-15	45.60%
GAWL01039561	P82596.3	plc_halla ame: full=perlucin	1132	1	3.50E-08	43.00%
GAWL01039562	P82596.3	plc_halla ame: full=perlucin	1825	5	4.10E-15	45.00%
GAWL01039942	P82596.3	plc_halla ame: full=perlucin	862	4	6.00E-12	42.25%
GAWL01039949	P82596.3	plc_halla ame: full=perlucin	1310	4	2.30E-11	42.50%
GAWL01039955	P82596.3	plc_halla ame: full=perlucin	2061	4	4.50E-11	42.50%
GAWL01040005	P82596.3	plc_halla ame: full=perlucin	3161	1	2.60E-10	53.00%
GAWL01040014	P82596.3	plc_halla ame: full=perlucin	697	1	1.40E-09	50.00%
GAWL01040017	P82596.3	plc_halla ame: full=perlucin	288	1	9.90E-07	46.00%
GAWL01040019	P82596.3	plc_halla ame: full=perlucin	3173	1	1.30E-08	50.00%
GAWL01039998	P82596.3	plc_halla ame: full=perlucin	276	1	8.10E-09	48.00%
GAWL01040001	P82596.3	plc_halla ame: full=perlucin	685	2	1.60E-11	45.50%
GAWL01040059	P82596.3	plc_halla ame: full=perlucin	1279	2	1.60E-07	41.50%
GAWL01040060	P82596.3	plc_halla ame: full=perlucin	1261	2	1.60E-07	41.50%
GAWL01040061	P82596.3	plc_halla ame: full=perlucin	1174	2	1.50E-07	41.50%
GAWL01041133	P82596.3	plc_halla ame: full=perlucin	517	1	8.20E-10	46.00%
GAWL01041471	P82596.3	plc_halla ame: full=perlucin	688	7	8.80E-21	44.57%
GAWL01041836	P82596.3	plc_halla ame: full=perlucin	477	7	1.40E-24	47.86%
GAWL01042285	P82596.3	plc_halla ame: full=perlucin	454	4	8.00E-14	47.25%
GAWL01042962	P82596.3	plc_halla ame: full=perlucin	218	1	9.20E-07	47.00%
GAWL01043044	P82596.3	plc_halla ame: full=perlucin	321	2	5.70E-11	55.50%
GAWL01043334	P82596.3	plc_halla ame: full=perlucin	362	4	2.80E-11	48.25%
GAWL01044009	P82596.3	plc_halla ame: full=perlucin	240	1	1.80E-07	48.00%
GAWL01044290	P82596.3	plc_halla ame: full=perlucin	241	2	7.70E-08	47.00%
GAWL01000825	P82596.3	plc_halla ame: full=perlucin	360	6	8.50E-21	46.33%
GAWL01000833	P82596.3	plc_halla ame: full=perlucin	276	4	2.80E-11	50.50%
GAWL01000834	P82596.3	plc_halla ame: full=perlucin	261	3	4.00E-11	50.67%
GAWL01000956	P82596.3	plc_halla ame: full=perlucin	521	7	2.40E-19	42.71%

GAWL01001767	P82596.3	plc_halla ame: full=perlucin	508	6	1.20E-18	45.50%
GAWL01001859	P82596.3	plc_halla ame: full=perlucin	1307	2	3.30E-11	40.00%
GAWL01002083	P82596.3	plc_halla ame: full=perlucin	701	1	9.50E-12	50.00%
GAWL01002281	P82596.3	plc_halla ame: full=perlucin	301	6	1.10E-12	49.33%
GAWL01002295	P82596.3	plc_halla ame: full=perlucin	587	7	3.80E-19	45.00%
GAWL01002403	P82596.3	plc_halla ame: full=perlucin	1122	3	1.10E-10	44.00%
GAWL01003008	P82596.3	plc_halla ame: full=perlucin	385	1	8.30E-07	55.00%
GAWL01003137	P82596.3	plc_halla ame: full=perlucin	638	7	3.10E-19	45.29%
GAWL01003334	P82596.3	plc_halla ame: full=perlucin	629	3	6.50E-10	42.33%
GAWL01003381	P82596.3	plc_halla ame: full=perlucin	314	4	2.50E-11	51.75%
GAWL01003468	P82596.3	plc_halla ame: full=perlucin	808	7	2.00E-18	45.14%
GAWL01004537	P82596.3	plc_halla ame: full=perlucin	307	4	8.50E-12	49.75%
GAWL01005212	P82596.3	plc_halla ame: full=perlucin	711	3	1.70E-15	42.33%
GAWL01021489	P84811.1	pwap_halla ame: full=perlwapin	323	1	6.70E-07	55.00%
GAWL01005863	ABS19815.1	sarco endoplasmic reticulum calcium atpase isoform a	5424	3	0.00E+00	75.33%
GAWL01026599	ABS19815.1	sarco endoplasmic reticulum calcium atpase isoform a	3567	3	7.60E-93	47.67%
GAWL01026600	ABS19815.1	sarco endoplasmic reticulum calcium atpase isoform a	1501	3	7.10E-40	55.33%
GAWL01004710	ABX57736.1	tfg beta signaling pathway factor	384	1	9.70E-13	84.00%
GAWL01031629	BAF42771.1	tyrosinase-like protein 1	813	3	1.10E-37	47.33%
GAWL01031630	BAF42771.1	tyrosinase-like protein 1	2403	3	3.20E-35	48.00%
GAWL01031631	BAF42771.1	tyrosinase-like protein 1	2430	3	3.30E-35	48.00%
GAWL01031633	BAF42771.1	tyrosinase-like protein 1	2403	3	3.20E-35	48.00%
GAWL01031635	BAF42771.1	tyrosinase-like protein 1	2430	3	3.30E-35	48.00%
GAWL01004918	BAF42772.1	tyrosinase-like protein 2	390	3	8.20E-14	45.67%
GAWL01018228	JH815923.1	Differentially or highly expressed in Crassostrea gigas mantle tissue	2008	1	1.00E-30	83.00%
GAWL01017748	JH816073.1	Differentially or highly expressed in Crassostrea gigas mantle tissue	979	1	1.40E-21	85.00%
GAWL01045091	JH816168.1	Differentially or highly expressed in Crassostrea gigas mantle tissue	307	1	1.10E-27	80.00%
GAWL01000001	JH816168.1	Differentially or highly expressed in Crassostrea gigas	207	1	4.20E-40	81.00%

		mantle tissue				
GAWL01012116	JH816189.1	Differentially or highly expressed in Crassostrea gigas mantle tissue	349	1	4.50E-42	91.00%
GAWL01012117	JH816189.1	Differentially or highly expressed in Crassostrea gigas mantle tissue	766	1	8.60E-167	80.00%
GAWL01019644	JH816189.1	Differentially or highly expressed in Crassostrea gigas mantle tissue	676	1	3.60E-150	80.00%
GAWL01024987	JH816189.1	Differentially or highly expressed in Crassostrea gigas mantle tissue	979	3	1.10E-146	78.00%
GAWL01019441	JH816585.1	Differentially or highly expressed in Crassostrea gigas mantle tissue	505	1	1.90E-12	76.00%
GAWL01019442	JH816585.1	Differentially or highly expressed in Crassostrea gigas mantle tissue	487	1	1.90E-12	76.00%
GAWL01012989	JH816769.1	Differentially or highly expressed in Crassostrea gigas mantle tissue	307	2	3.80E-62	82.00%
GAWL01021618	JH816843.1	Differentially or highly expressed in Crassostrea gigas mantle tissue	2885	1	3.10E-32	84.00%
GAWL01007983	JH816852.1	Differentially or highly expressed in Crassostrea gigas mantle tissue	1202	1	1.00E-23	93.00%
GAWL01012990	JH816866.1	Differentially or highly expressed in Crassostrea gigas mantle tissue	307	2	2.30E-69	82.50%
GAWL01011674	JH816980.1	Differentially or highly expressed in Crassostrea gigas mantle tissue	447	1	3.30E-84	85.00%
GAWL01026283	JH816980.1	Differentially or highly expressed in Crassostrea gigas mantle tissue	639	1	5.10E-39	80.00%
GAWL01003177	JH817066.1	Differentially or highly expressed in Crassostrea gigas mantle tissue	373	1	1.10E-23	85.00%
GAWL01024988	JH817078.1	Differentially or highly expressed in Crassostrea gigas mantle tissue	939	1	1.60E-75	76.00%
GAWL01038785	JH817078.1	Differentially or highly expressed in Crassostrea gigas mantle tissue	2093	3	0.00E+00	81.67%
GAWL01038794	JH817078.1	Differentially or highly expressed in Crassostrea gigas mantle tissue	2036	3	0.00E+00	81.67%
GAWL01038795	JH817078.1	Differentially or highly expressed in Crassostrea gigas mantle tissue	2489	3	0.00E+00	82.00%
GAWL01038787	JH817078.1	Differentially or highly expressed in Crassostrea gigas mantle tissue	768	2	1.50E-134	85.00%

GAWL01038788	JH817078.1	Differentially or highly expressed in Crassostrea gigas mantle tissue	1851	3	0.00E+00	82.00%
GAWL01038789	JH817078.1	Differentially or highly expressed in Crassostrea gigas mantle tissue	1951	3	0.00E+00	81.67%
GAWL01038791	JH817078.1	Differentially or highly expressed in Crassostrea gigas mantle tissue	2159	3	0.00E+00	82.00%
GAWL01038793	JH817078.1	Differentially or highly expressed in Crassostrea gigas mantle tissue	865	2	2.90E-127	84.00%
GAWL01018747	JH817228.1	Differentially or highly expressed in Crassostrea gigas mantle tissue	3644	1	3.10E-13	89.00%
GAWL01006995	JH817484.1	Differentially or highly expressed in Crassostrea gigas mantle tissue	1707	1	6.80E-07	92.00%
GAWL01013936	JH817484.1	Differentially or highly expressed in Crassostrea gigas mantle tissue	379	1	2.30E-30	89.00%
GAWL01002045	JH817532.1	Differentially or highly expressed in Crassostrea gigas mantle tissue	356	1	1.30E-12	100.00%
GAWL01002046	JH817532.1	Differentially or highly expressed in Crassostrea gigas mantle tissue	307	1	1.10E-12	100.00%
GAWL01040644	JH817704.1	Differentially or highly expressed in Crassostrea gigas mantle tissue	1214	1	3.70E-08	92.00%
GAWL01016929	JH817738.1	Differentially or highly expressed in Crassostrea gigas mantle tissue	1148	1	1.20E-22	84.00%
GAWL01011647	JH817782.1	Differentially or highly expressed in Crassostrea gigas mantle tissue	1221	1	8.00E-15	82.00%
GAWL01012118	JH817877.1	Differentially or highly expressed in Crassostrea gigas mantle tissue	402	2	5.40E-27	83.00%
GAWL01016301	JH817892.1	Differentially or highly expressed in Crassostrea gigas mantle tissue	2254	1	9.00E-12	89.00%
GAWL01028947	JH818313.1	Differentially or highly expressed in Crassostrea gigas mantle tissue	1372	1	0.00E+00	79.00%
GAWL01028957	JH818313.1	Differentially or highly expressed in Crassostrea gigas mantle tissue	1871	1	0.00E+00	84.00%
GAWL01028959	JH818313.1	Differentially or highly expressed in Crassostrea gigas mantle tissue	1981	1	0.00E+00	79.00%
GAWL01028961	JH818313.1	Differentially or highly expressed in Crassostrea gigas mantle tissue	1026	1	0.00E+00	84.00%
GAWL01028964	JH818313.1	Differentially or highly expressed in Crassostrea gigas mantle tissue	1626	1	0.00E+00	78.00%

GAWL01028965	JH818313.1	Differentially or highly expressed in Crassostrea gigas mantle tissue	1928	1	0.00E+00	79.00%
GAWL01028948	JH818313.1	Differentially or highly expressed in Crassostrea gigas mantle tissue	1386	1	0.00E+00	79.00%
GAWL01028966	JH818313.1	Differentially or highly expressed in Crassostrea gigas mantle tissue	1558	1	0.00E+00	84.00%
GAWL01028967	JH818313.1	Differentially or highly expressed in Crassostrea gigas mantle tissue	1967	1	0.00E+00	79.00%
GAWL01028969	JH818313.1	Differentially or highly expressed in Crassostrea gigas mantle tissue	1615	1	0.00E+00	83.00%
GAWL01028970	JH818313.1	Differentially or highly expressed in Crassostrea gigas mantle tissue	1615	1	0.00E+00	79.00%
GAWL01028949	JH818313.1	Differentially or highly expressed in Crassostrea gigas mantle tissue	1036	1	3.00E-38	82.00%
GAWL01028950	JH818313.1	Differentially or highly expressed in Crassostrea gigas mantle tissue	1884	1	0.00E+00	85.00%
GAWL01028951	JH818313.1	Differentially or highly expressed in Crassostrea gigas mantle tissue	1571	1	0.00E+00	84.00%
GAWL01028952	JH818313.1	Differentially or highly expressed in Crassostrea gigas mantle tissue	1039	1	0.00E+00	84.00%
GAWL01028953	JH818313.1	Differentially or highly expressed in Crassostrea gigas mantle tissue	1928	1	0.00E+00	84.00%
GAWL01028954	JH818313.1	Differentially or highly expressed in Crassostrea gigas mantle tissue	1612	1	0.00E+00	78.00%
GAWL01028955	JH818313.1	Differentially or highly expressed in Crassostrea gigas mantle tissue	1083	1	2.60E-178	83.00%
GAWL01002076	JH818820.1	Differentially or highly expressed in Crassostrea gigas mantle tissue	3432	1	1.30E-36	85.00%
GAWL01001009	JH818839.1	Differentially or highly expressed in Crassostrea gigas mantle tissue	1082	1	2.60E-09	77.00%

951